Quaternary Research (2025), 1–31
doi:10.1017/qua.2024.51

Research Article

Late Pleistocene pedogenesis and loess magnetism in northwestern Ukraine

Oleksandr Bonchkovskyi[a,b] and Dmytro Hlavatskyi[c,d]

[a]Taras Shevchenko National University of Kyiv, Volodymyrska Str., 60, 02000 Kyiv, Ukraine; [b]Institute of Geography, National Academy of Sciences of Ukraine, Volodymyrska Str., 44, 01130 Kyiv, Ukraine; [c]Institute of Geophysics, National Academy of Sciences of Ukraine, Akademika Palladina Av. 32, 03142 Kyiv, Ukraine and [d]Institute of Geophysics, Polish Academy of Sciences, Księcia Janusza 64, 01-452 Warsaw, Poland

Abstract

The central European loess-paleosol sequence (Marine Oxygen Isotope Stage (MIS) 6–2) at three sites located in northwestern Ukraine, in the transitional area between the oceanic and continental climates, has been studied using micromorphological, grain-size, pollen, and magnetic methods. The sequence is characterized by a well-developed pedocomplex S1 (correlative of MIS 5), comprising four soils, and three interstadial soils within loess L1 (MIS 4–2). The soils of S1 are synsedimentary, indicating a dynamic depositional environment with pulses of aeolian sand sedimentation from late MIS 6 to MIS 5a. From various cryogenic features, the permafrost aggradation for MIS 6, 4, and 2, and deep seasonal freezing for MIS 5d and 5b were reconstructed. Distinct redoximorphic features of the loess units, widespread solifluction, well-developed periglacial phenomena, and very low magnetic susceptibility values for the loess-paleosol sequence of northwestern Ukraine reveal its similarity to those of the central European loess subdomain of the northern European loess belt. The low concentration of ferrimagnetic minerals in the parent material and intensive processes of physical and chemical weathering are reflected in the specific model of magnetic enhancement of the studied sequence, which is transitional between the "Chinese" (pedogenic) and "Alaskan" (reducing-pedogenic) models.

Keywords: Loess-paleosol sequence, paleosol, soil micromorphology, magnetic susceptibility, rock magnetism, Volyn Upland, Ukraine, paleoenvironmental reconstructions

Introduction

Among terrestrial paleoenvironmental archives, loess-paleosol sequences (LPSs) preserve detailed records of Quaternary climate fluctuations. Paleosols were mainly formed into loess material under warmer and more humid climatic conditions during interglaciations, and loess generally accumulated under cold and dry conditions during glacial periods (Kukla, 1977; Pécsi, 1990; Pye, 1995; Bronger, 2003; Lowe and Walker, 2014; Li et al., 2020).

From a paleopedological point of view, the northwestern Ukrainian loess region is of particular interest because of its transitional character between the central and eastern European subdomains in the northern European loess belt (Lehmkuhl et al., 2021; Matoshko, 2021). On the other hand, during the Pleistocene, northwestern Ukraine was located within an ecotone (forest/steppe), which determined the high sensitivity of the loess accumulation to global and regional paleoclimatic signals, resulting in a detailed stratigraphy of various LPSs and a high diversity of paleosol types. Moreover, the LPSs of this region are considered to be a valuable record of Pleistocene cryogenesis (Bogucki, 1986; Jary, 2009).

The Upper Pleistocene LPSs of the northern European loess belt have been comprehensively studied by many authors (Veklych, 1968, 1982; Kukla and Cílek, 1996; Becze-Deàk et al., 1997; Rousseau et al., 2001; Haesaerts et al., 2003, 2016; Gerasimenko, 2006; Antoine et al., 2013, 2016; Sprafke et al., 2013; Gocke et al., 2014; Łanczont et al., 2015; Hošek et al., 2015, 2017; Matviishyna and Kushnir, 2021; Adameková et al., 2021; Bradák et al., 2021a; Bertran et al., 2022). Micromorphology has been applied as a particular tool for reconstructing the pedogenic processes, revealing the phases of pedogenesis and diagenetic soil transformation (Fedoroff and Goldberg, 1982; Matviishyna, 1982; Rose et al., 2000; Mroczek, 2013; Solleiro-Rebolledo et al., 2013; Sprafke et al., 2014; Makeev et al., 2024). Despite the value of paleosol studies, insufficient attention has been paid to the evolution of pedogenic processes and the classification of paleosols, in particular in the LPSs of northwestern Ukraine. Therefore, some problems arise regarding the genetic interpretation of paleosols (Kemp, 2001), particularly the classification of paleosols, identification of primary and secondary soil characteristics, soil welding, secondary soil erosion, etc.

The synthesis of rock magnetic and pedogenic data in LPSs has yielded valuable paleoenvironmental interpretations (Tsatskin

Corresponding author: Oleksandr Bonchkovskyi; Email: geobos2013@gmail.com
Cite this article: Bonchkovskyi O, Hlavatskyi D (2025). Late Pleistocene pedogenesis and loess magnetism in northwestern Ukraine. *Quaternary Research* 1–31. https://doi.org/10.1017/qua.2024.51

et al., 1998, 2008; Terhorst et al., 2001; Maher et al., 2003; Marković et al., 2008, 2011, 2018; Maher, 2016; Sümegi et al., 2018; Wacha et al., 2018; Bradák et al., 2019; Gerasimenko et al., 2022). Magnetic susceptibility (χ) and its frequency dependence ($\chi_{fd\%}$) are useful paleoenvironmental proxies (Heller et al., 1991; Maher and Thompson, 1992; Forster et al., 1994; Dearing et al., 1996; Liu et al., 1999; Evans and Heller, 2001). The latter is a direct result of the soil-forming processes and the formation of magnetic minerals during pedogenesis (Maher, 1998). Other rock magnetic parameters are widely used to identify the concentration, composition, and grain size of magnetic minerals, which are sensitive to environmental change (Evans and Heller, 2003; Maxbauer et al., 2016). The application of these parameters in Eurasian loess studies has been extended in recent years (Dzierżek et al., 2020; Bradák et al., 2021b; Jordanova and Jordanova, 2021; Költringer et al., 2021a, 2021b; Laag et al., 2021; Namier et al., 2021; Wacha et al., 2021; Zeeden and Hambach, 2021; Jordanova et al., 2022; Ghafarpour et al., 2023; Guo et al., 2023; Aquino et al., 2024; Marković et al., 2024).

Only two loess-paleosol sections in northwestern Ukraine, Boyanychi and Korshiv, have been studied using techniques of rock magnetism (Nawrocki et al., 1996; Bakhmutov et al., 2017) and paleomagnetism (Nawrocki et al., 1999; Hlavatskyi et al., 2016; for a comprehensive overview, see Bakhmutov et al., 2023). However, some important magnetic parameters (such as $\chi_{fd\%}$) from these studies are lacking, as well as a comparison of rock magnetic indices and paleopedological characteristics.

The loess sequence at the Smykiv, Novyi Tik, and Kolodezhi sites is a promising loess-paleosol sequence for paleopedological and magnetic studies since it is represented by well-developed paleosols. This paper aims to present a multiproxy study of the sequence and discuss its significance for understanding short-term changes in pedogenesis, sedimentation, and environmental impacts on the rock magnetic record in the Late Pleistocene. In particular, the changes in pedogenesis and their link to sedimentation, as well as the classification of paleosols using field observations, micromorphology, and grain-size analysis are distinguished. Since there are many paleocryogenic features, we shed new light on paleocryogenic events and the conditions under which cryogenic structures were formed. In addition, we apply different models of magnetic enhancement and dissolution in LPSs and propose a new transitional mechanism for the formation of magnetic properties in the studied region. Ultimately, the obtained paleopedological, paleocryological, and magnetic data should refine the scheme of paleoenvironmental changes during the Late Pleistocene in the transitional zone between central and eastern Europe, i.e., between areas with oceanic and continental climates.

Geologic background

The LPSs of northwestern Ukraine have been extensively studied since the 1960s (Bogucki et al., 1975, 2014; Morozova, 1981; Bogucki, 1986; Nawrocki et al., 1996, 2006, 2018; Bogucki and Voloshyn, 2008, 2014; Jary, 2009; Bezusko et al., 2011; Kusiak et al., 2012; Fedorowicz et al., 2013; Jary and Ciszek, 2013; Hlavatskyi et al., 2016; Bonchkovskyi, 2020a, 2020b; Bonchkovskyi et al., 2023a, 2023b, and others). The LPSs of western Ukraine were examined using the local stratigraphic scheme of western Ukraine developed by A. Bogucki (1986) and subsequently modified by Łanczont and Boguckyj (2007) and Bogucki et al. (2014).

In this scheme, the Upper Pleistocene comprises a well-developed bipartite pedocomplex (Horokhiv unit, S1) overlain by a thick loess (L1) with three recognizable interstadial Gleysols (Krasyliv, Rivne, and Dubno units) associated with cryogenic levels (Bogucki, 1986). The Horokhiv pedocomplex (S1) consists of a lower interglacial soil with a pronounced Bt horizon and an upper interstadial humified soil (Morozova, 1981; Bogucki, 1986). In the most complete sections, the upper humified soil has been divided into three separate humified soils affected by solifluction and designated as the Kolodiiv soils (Łanczont and Boguckyj, 2007; Łanczont et al., 2015, 2022). Based on numerous optically stimulated luminescence and thermoluminescence dates at Korshiv, Boyanychi, Pronyatyn, Yezupil, and other sites, the Horokhiv soil complex was correlated with the entire Marine Oxygen Isotope Stage (MIS) 5 (Łanczont et al., 2023).

The Dubno unit (L1S1) in the LPSs of western Ukraine is predominantly represented by Gleysol (Morozova, 1981; Bogucki, 1986; Łanczont and Boguckyj, 2007; Kusiak et al., 2012; Fedorowicz et al., 2013; Jary and Ciszek, 2013; Bogucki et al., 2014; Łanczont and Madeyska, 2015). Brown soils were described only in some sections in Poland (Jary and Ciszek, 2013) and in Subcarpathia (Łącka et al., 2007) where they are represented by a set of interstadial soils. In numerous studies, the Dubno unit has been correlated with MIS 3 (Łanczont and Boguckyj, 2007; Fedorowicz et al., 2013, 2018; Jary and Ciszek, 2013).

The Rivne unit (L1-s2/l1) is a moderately developed Gleysol affected by solifluction and occasional ice-wedge pseudomorphs, whereas the Krasyliv unit (L1-s1/l1) is considered to be a buried active layer and is associated with the largest ice-wedge pseudomorphs (Bogucki et al., 1975; Nechaev, 1983; Bogucki, 1986; Fedorowicz et al., 2018).

In this study, we use the Quaternary stratigraphic framework of Ukraine (Veklych, 1968; 1982; Veklych et al., 1993) and its modifications by Gerasimenko (2004), Gozhik et al. (2000, 2014), and Matviishyna et al. (2010), which are widely applied to the LPSs in other regions of Ukraine. In this scheme, each chronostratigraphic unit was named after its stratotype locality, and its index consists of two letters (e.g., Pryluky, "pl"). Each pedocomplex may include soils of the initial (designated by index "a"), optimal (designated "b"), and final (designated "c") phases of pedogenesis. Usually, two middle "b" soils (marked as "b1" and "b2") are well defined and correspond to more pronounced climatic optima. Soils of the initial and final phases, "a" and "c," show signs of development under cooler climates. Stages covering two to three climatic optima (usually, they correspond to interstadial or interglacial periods) are designated by odd numbers, e.g., Lower Pryluky, "pl_1," Upper Pryluky, "pl_3." Even numbers indicate cold stages (stadial and glacial periods), e.g., Middle Pryluky, "pl_2."

The correlation of the two stratigraphic frameworks has been the subject of debate in recent decades owing to different chronological interpretations of these schemes (Gerasimenko, 2004; Lindner et al., 2006; Łanczont and Boguckyj, 2007; Bogucki et al., 2009, 2012; Matviishyna et al., 2010; Bonchkovskyi, 2020a; Łanczont et al., 2022); however, the names of the stratotypes and units remain constant. The correlation issues will be considered in the "Discussion" section.

Study area

The study area is the Volyn Upland (Fig. 1), where three LPSs were investigated, namely: Smykiv, Novyi Tik, and Kolodezhi (Fig. 2). The Smykiv (50°28.18′N, 25°08.22′E) and Kolodezhi

https://doi.org/10.1017/qua.2024.51 Published online by Cambridge University Press

Figure 1. (A) Location of the study area on the map of loess distribution at the regional and (B) European scale. Loess distribution is mapped as in Lehmkuhl et al. (2021). I. Weichselian marginal and protogenetic zone: Ia, western protogenetic subdomain; Ib, eastern protogenetic subdomain. II. Northern European loess belt: IIc, central European continental subdomain; IId, eastern European continental subdomain. III. Loess adjacent to central European and high-altitude mountain range: IIId, eastern margin of the European Alps and northern Carpathian Basin subdomain. V. Pontic East European domain. Loess-paleosol sequences: 1, Biały Kościół; 2, Paks; 3, Stari Slankamen; 4, Lunca; 5, Suhia Kladenetz; 6, Dolynske; 7, Stari Kaydaky.

(50°29.49′N, 25°05.34′E) sites are located on the right-bank slope of the Dezha river (middle and upper stream, respectively), and the Novyi Tik section (50°29.50′N, 25°12.17′E) is situated on the left-bank slope of the Berestova river. The Dezha river valley consists of a 200–400 m wide floodplain and fragments of the Upper Pleistocene river terrace that appear towards its mouth (Fig. 2). The Berestova river valley is similar to the Dezha river valley in size and geologic context. The Volyn Upland is characterized by an undulating relief (200–250 m above sea level) significantly dissected by branched dry valleys and gullies up to 3–5 km long (Fig. 2A). The Styr river valley, the main river of the study area, includes three river terraces of the Upper and Middle Pleistocene (Fig. 2B).

The regional loess-paleosol succession is underlain by Upper Cretaceous limestones, chalks, and marls with flint nodules. Beneath the Upper Cretaceous rocks, Devonian reddish sandstones and siltstones constitute a continuous formation (up to 2 km in thickness), overlying Silurian limestones, argillites, and siltstones (Gerenchuk, 1976).

The present-day climate is continental moderate. At the meteorological station in Lutsk (40 km north of the Smykiv section), the average annual temperature is +7.7°C, in January −4.0°C, and in July +18.8°C, and precipitation is 560 mm (Osadchyi et al., 2022). In the study area, the soil cover is varied, dominated by Haplic Luvisols, Luvic Phaeozems, Haplic Phaeozems, Luvic Chernozems, and Haplic Chernozems. Albic Luvisols, Calcic Chernozems, and Arenosols occupy isolated areas (Sharyfulina et al., 1967). Vegetation is mainly represented by agrocoenoses and meadows on the site of agricultural land. Natural vegetation is represented by oak–hornbeam forests on plateaus and meadow-steppe on the steep slopes of dry valleys and gullies.

Materials and methods

The stratigraphy of the Smykiv sequence was studied in four excavations located on different landforms (lower and upper slopes of the Dezha river valley). In excavations #1 and #2, all stratigraphic units were exposed (Fig. 3), whereas in excavation #3 only the upper part of the section was studied. Excavation #4 was dug out on the lower slope of the Dezha river valley, which resulted in mixed and strongly disturbed sediments that hampered preservation of stratification.

All genetic horizons of the investigated paleosols were studied in accordance with the "Guidelines for Soil Descriptions" (FAO, 2006). Field interpretation of paleosols was performed according to IUSS Working Group WRB (2022). The soil color was

https://doi.org/10.1017/qua.2024.51 Published online by Cambridge University Press

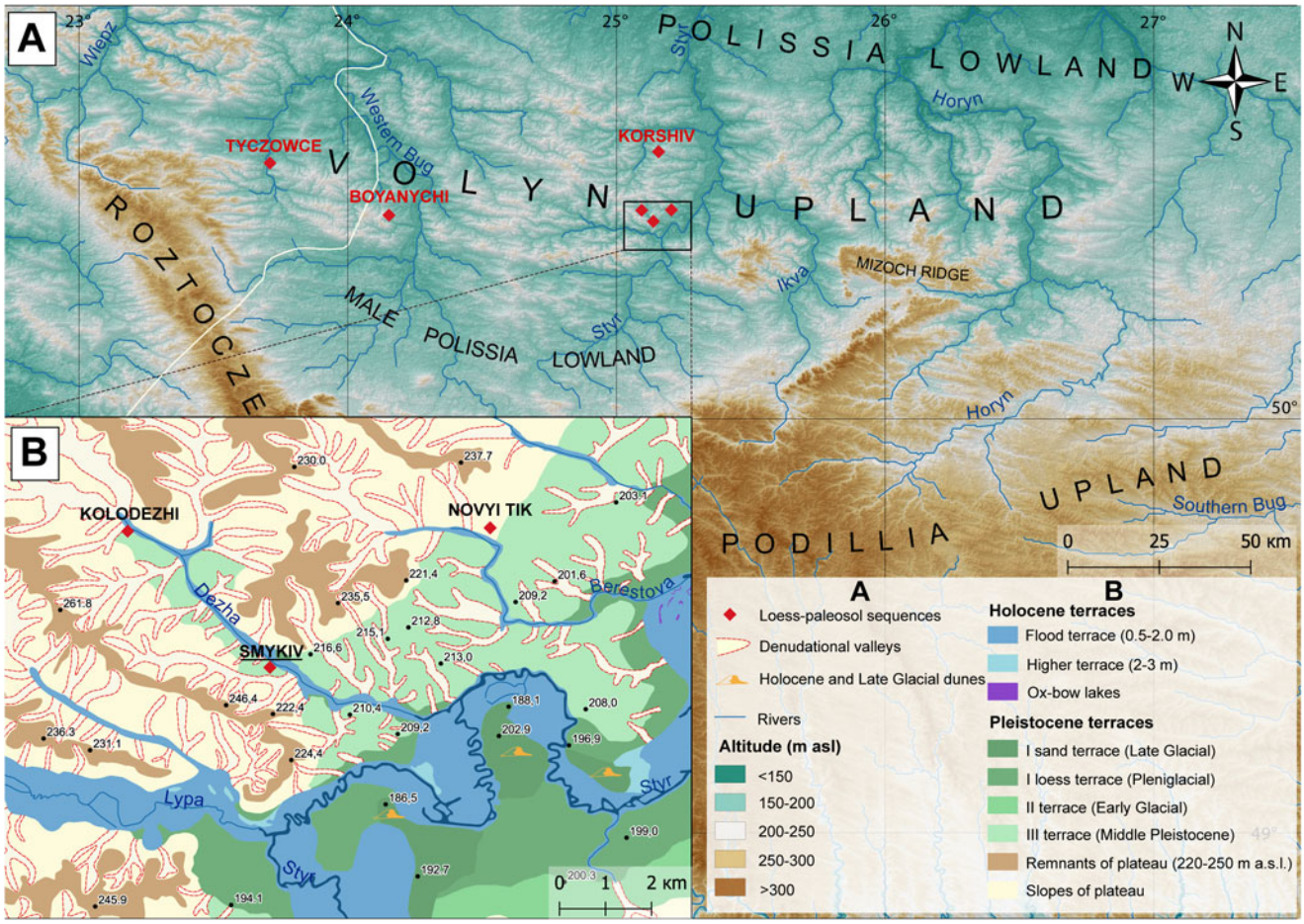

Figure 2. (A) Relief of northwestern Ukraine; the map is created based on the Shuttle Radar Topography Mission Digital Elevation Model 1 Arc-Second (NASA Shuttle Radar Topography Mission (SRTM), 2013). (B) Geomorphological map of the central part of the Volyn Upland.

determined according to the Munsell soil color chart (Munsell Color, 2009). Eighteen samples for micromorphological and grain-size analysis were taken in 2019 from each genetic horizon of the paleosols and from each bed of the non-soil deposits. Excavations #1 and #2 were subjected to sampling because of their completeness. Micromorphological features of paleosols were described according to the terminology of Stoops (2003) and Stoops et al. (2018).

Grain size was measured in the Laboratory of Landscape Ecology at the Taras Shevchenko National University of Kyiv according to the pipette method (Kachynskyi, 1958), recording the following fractions: <1 μm (clay), 2–5 μm (very fine silt), 5–10 μm (fine silt), and 10–50 μm (coarse silt). The content of coarse fractions (50–250 μm, 250–500 μm, 500–1000 μm, and >1000 μm) was determined by sieving. Grain-size parameters such as median (Md) and average particle radius (Mz) were calculated as in Folk and Ward (1957) and presented in phi (φ). The sorting index was calculated according to Trask (1932). The loess (Kd) index (10–50 μm/<5 μm) is applied in this paper according to Jary (2007). To estimate the relationship between pedogenesis and sedimentation, the soil/sedimentation (SSI) index according to Bonchkovskyi et al. (2023b) was applied.

Another collection of samples for magnetic measurements was taken at Smykiv in 2022. In total, 130 powder samples from the depth interval between 0.05 and 6.25 m (with a step of 5 cm) were extracted, including three additional samples from the largest ice-wedge pseudomorph (Fig. 3). Magnetic measurements were carried out in the laboratory of the Institute of Geophysics of the National Academy of Sciences of Ukraine (Demydiv).

To obtain a high-resolution magnetic susceptibility record, samples with a mass of about 10 g were prepared. Measurements of mass-specific susceptibility were carried out at the dual frequencies of 976 Hz (χ_{lf}; used as standard magnetic susceptibility quantity) and 15,616 Hz (χ_{hf}) using a MFK1-FB Kappabridge. The differences between the two susceptibilities provided the frequency-dependent magnetic susceptibility. The absolute (χ_{fd}) and its relative parameter ($\chi_{fd\%}$) were calculated as follows: $\chi_{fd} = \chi_{lf} - \chi_{hf}$; $\chi_{fd\%} = (\chi_{lf} - \chi_{hf})/\chi_{lf} \times 100$

Isothermal remanent magnetization (IRM) curves were obtained for 15 specimens from all stratigraphic units in magnetic fields from 0 to 1.0 T. The following magnetic parameters were measured for a pilot collection of 65 samples: (1) anhysteretic remanent magnetization (ARM) produced along one spatial axis and induced with a 50 μT static field and 50 mT alternating field using an AMU-1A anhysteretic magnetizer; (2) saturation isothermal remanent magnetization (IRM_{1T}) acquired under a magnetic field of 1.0 T; and (3) $IRM_{-0.3T}$ acquired under the opposite magnetic field of −300 mT. The anhysteretic susceptibility (χ_{ARM}) was calculated by dividing the ARM by the direct current magnetic field (~0.04 mT in Demydiv). Combinations of

https://doi.org/10.1017/qua.2024.51 Published online by Cambridge University Press

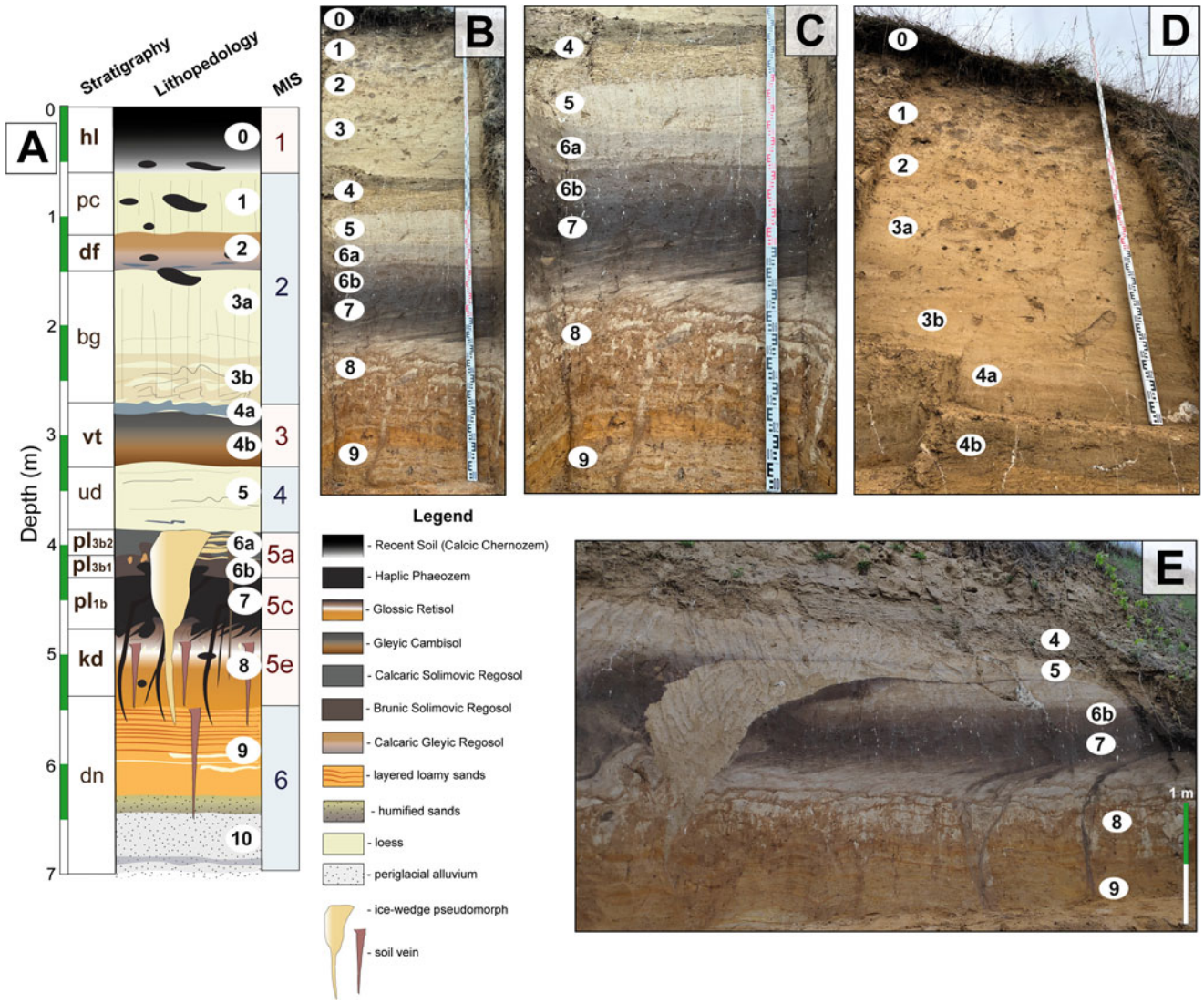

Figure 3. (A) Stratigraphy of the Smykiv sequence. (B) Section #1 (year 2017). (C) Lower part of section #1 (year 2017). (D) Upper part of section #1 (year 2017). (E) Section #2 (year 2019). See Table 1 for definition of stratigraphic units.

these parameters were used to calculate rock magnetic ratios: granulometric indices ARM/IRM_{1T}, χ_{ARM}/χ_{lf}, and IRM_{1T}/χ_{lf}; indices of magnetic hardness $S = IRM_{-0.3T}/IRM_{1T}$ and $HIRM = (IRM_{1T} + IRM_{-0.3T})/2$ (Evans and Heller, 2003; Maxbauer et al., 2016).

To complement regional paleoenvironmental reconstructions, new palynological data from the nearby Kolodezhi site were used, as well as paleopedological, palynological, and geochemistry records from previously studied Volyn Upland sequences, e.g., Novyi Tik (Bonchkovskyi, 2020a; Bonchkovskyi et al., 2023a, 2023b). The paleoenvironmental reconstructions were enhanced by a comparison of our pollen data with formerly studied LPSs of western Ukraine and Poland. Pollen analysis of eight samples from the Kolodezhi section was prepared according to the following technique: boiling in a 10% HCl solution to remove carbonates; boiling in a $Na_4P_2O_7$ solution to remove clay particles; boiling in HCl to remove secondary carbonates; boiling in a 10% KOH solution to remove organic matter; separation in a heavy liquid (CdI_2 + KI) with the specific gravity 2.0–2.2; and, finally, treatment with a 40% HF solution to remove quartz grains.

Results

Stratigraphic subdivision

The loess-paleosol sequence at Smykiv comprises 13 stratigraphic units: six paleosols and seven non-soil beds (Fig. 3). A short description of the soils is given in Table 1. The correlation of units of the Quaternary stratigraphic framework of Ukraine, stratigraphic scheme of western Ukraine, and marine isotope stages is explained in the "Discussion" section.

The lowermost unit in the Smykiv section, Dnipro (layers 9–10, MIS 6), is represented by thick (over 5 m) laminated loamy sands with several levels affected by cryoturbation that enabled an interpretation of these sediments as periglacial alluvium. The alluvium is overlain by humified sands with horizontal and wavy lamination, in which lenses with bleached coarse-grained sands are present. Reddish sands interbedded with grey gleyed loams lie above and underwent significant secondary pedogenesis influence, which led to their acquisition of prismatic structures and clay coatings on the ped surfaces.

https://doi.org/10.1017/qua.2024.51 Published online by Cambridge University Press

Table 1. Morphological description of the Smykiv stratigraphic units.

Layer	Unit	Subunit	MIS	Depth (m)	Genetic horizons	Description	Interpretation
0	Holocene (hl)		1	0.0–0.3	Ahp	N 4/0, silt loam, truncated, friable, with granular structure.	Calcic Chernozem (Siltic, Aric, Humic)
				0.3–0.6	Bk	10YR 6/2, silt loam, firm, with subangular blocky structure, dispersed powdery lime and numerous krotovinas.	
1	Prychornomorya (pc)		2	0.6–1.2	Ck	10YR 8/1, silt loam, strongly calcareous (dispersed powdery lime, pseudomycelia, soft and hard carbonate nodules), friable, with many krotovinas.	Loess
2	Dofinivka (df)	1b		1.2–1.35	2Awkb	5YR 7/4, silt loam, firm, moderately calcareous (dispersed powdery lime, pseudomycelia).	Calcaric Gleyic Regosol (Siltic, Ochric)
				1.35–1.5	2Bgkb	10YR 7/1, silt clay loam, firm, moderately calcareous (dispersed powdery lime, pseudomycelia), slightly mottled (redox depletion mottles).	
3a	Bug (bg)			1.5–2.3	Ckb	7.5YR 8/1, silt loam, firm, moderately calcareous (dispersed powdery lime, pseudomycelia, hard nodules).	Loess
3b				2.3–2.4	Ckgb	7.5YR 8/2 (loess material) and 10YR 7/4 (soil material), silt loam, friable, moderately calcareous (dispersed powdery lime, pseudomycelia, hard nodules, rhizoliths).	Solifluction/ pedosediment?
4a	Vytachiv (vt)	c	3	2.6–2.7	3Ag@b	10YR 6/1, silt loam, firm, moderately calcareous (pseudomycelia and cracks infilled with calcium carbonate).	Gleyic Regosol (Siltic, Protocalcic, Turbic)
4b		b		2.7–2.95	4Agb	7.5YR 5/1, silt loam, firm, with a platy structure, slightly calcareous (pseudomycelia, hard nodules, and cracks infilled with calcium carbonate). Many Fe–Mn pedofeatures.	Gleyic Cambisol (Siltic, Protocalcic, Ochric, Turbic)
				2.95–3.2	4Bwb	10YR 6/4, silt loam, slightly layered, very firm, with platy structure, slightly calcareous (pseudomycelia, soft nodules, and cracks infilled with calcium carbonate).	
5a	Uday (ud)		4	3.2–3.5	Ckgb	10YR 8/3, silt loam, firm, moderately calcareous (soft nodules and rhizoliths), with many Fe–Mn pedofeatures.	Loess
5b				3.5–3.8	Ck@b	Layered, 7.5YR 7/2 (loess material) and 7.5YR 7/1 (soil material), silt loam, firm, with weak platy structure, moderately calcareous (soft nodules and rhizoliths). Mn pedofeatures almost disappear, whereas Fe nodules appear. The lower boundary is erosional, abrupt.	Solifluction
6a	Upper Pryluky (pl_3)	3b2	5a	3.8–3.9	5Ak@b	10YR 6/1, loam, very firm, gleyed, with a weak platy structure, slightly calcareous (soft nodules and rhizoliths), with many Fe–Mn pedofeatures. The soil is significantly disturbed by solifluction. Earth worm burrows appear.	Calcaric Solimovic Regosol (Loamic, Ochric, Turbic)

(*Continued*)

https://doi.org/10.1017/qua.2024.51 Published online by Cambridge University Press

Table 1. (*Continued.*)

Layer	Unit	Subunit	MIS	Depth (m)	Genetic horizons	Description	Interpretation
				3.9–4.1	5Bwk@b	7.5YR 7/1, silt loam, firm, moderately calcareous (soft nodules and rhizoliths), with reticulate post-cryogenic texture accentuated by calcium carbonates. Fe–Mn pedofeatures almost disappear.	
6b		3b1		4.1–4.3	6Ab	7.5YR 5/1, loam, firm, slightly calcareous (soft nodules and rhizoliths), with elevated number of Fe–Mn pedofeatures.	Brunic Solimovic Regosol (Loamic, Protocalcic, Ochric)
7	Lower Pryluky (pl_1)	1b	5c	4.3–4.8	7Ah@b	7.5YR 3/1, silt loam, firm, with a weak granular structure, slightly calcareous (soft nodules and rhizoliths), significantly disturbed by solifluction and soil veins.	Haplic Phaeozem (Siltic, Humic, Solimovic, Turbic)
8	Kaydaky (kd)		5e	4.8–4.95	8AE@b	N 7/0, sandy loam, firm, with a weak platy structure, occasional carbonate rhizoliths and many Fe–Mn pedofeatures.	Albic Glossic Retisol (Loamic, Cutanic, Differentic, Lamellic)
				4.95–5.2	8EBt@b	N 8/0 and 10YR 7/4, sandy loam, friable, with cemented by Fe domains.	
				5.2–5.5	8Btg@b	10YR 6/2, silt loam, firm, with a moderate subangular blocky structure and SiO_2 powder on the ped surfaces. There are many Fe spots and pronounced reticulate post-cryogenic texture.	
9	Dnipro (dn)		6	5.5–6.4	Ctgb	10YR 7/4, sandy loam and loam, very firm, laminated, gleyed, with a moderate prismatic structure and reticulate post-cryogenic texture.	Aeolian sands?
10				6.4–7.0	Cb	10YR 7/1 and 10YR 7/3, loamy sand, laminated, with lenses of bleached sand.	Aeolian sands Alluvium
				7.0–9.0	C@b	10YR 8/2 and 10YR 7/8, loamy sand, with slightly convoluted lamination. There are many redoximorphic features, including Liesegang rings.	
				9.0–10.1	Cg@b	Mottled, loamy sand, with convoluted lamination and lenses of bleached sands. There are many Fe–Mn pedofeatures.	
				10.1–10.6	Cgb	7.5YR 7/1, sandy loam, with slightly convoluted lamination and Fe streaks.	
				10.6–11.4	Cg@b	Mottled, loam, with expressed loading structures and Fe streaks.	

The Kaydaky unit (layer 8, MIS 5e) is represented by a soil with distinct textural differences: the AE@b and EBt@b horizons are loamy sands, whereas the Btg@b horizon is a silt loam. Albeluvic glossae here penetrate the argic horizon, which, along with an abrupt textural difference, meet the criteria of a Retisol (IUSS Working Group WRB, 2022). The albic horizon is relatively thick (up to 0.4 m); however, in the upper part it is considerably humified; therefore, it is designated as the AE@b horizon, and in the lower part it alternates with reddish iron and clay-rich argic material; therefore, it is designated as the EBt@b horizon. In two upper horizons, a lenticular post-cryogenic texture occurs, accentuated by humified material. The argic horizon is characterized by clay coatings on the subangular blocky peds. Whitish silt cutans overlie the clay coatings. In the AE@b horizon, many small charcoal fragments and signs of mass-movement processes appear.

The Pryluky unit (layers 6 and 7, MIS 5a-c) directly overlies the Kaydaky unit. The Pryluky unit includes three relatively thin soils separated by cryogenic levels. The lower soil (layer 7, MIS 5c) is the darkest one in the section and is significantly deformed by soil veins and solifluction, which did not affect the overlying soil. Only secondary carbonates occur in the soil,

https://doi.org/10.1017/qua.2024.51 Published online by Cambridge University Press

including those that emphasize the reticulate post-cryogenic texture. Notably, krotovinas, abundant at this level in other sections (Bonchkovskyi, 2020a), are rare here. Thus, the soil is classified as a Haplic Phaeozem. The middle soil (layer 6b, MIS 5a) is very thin (15–25 cm) but clearly visible in the section as a humified soil, not affected by solifluction (Fig. 3C). The soil consists only of the Ab horizon and can be attributed to a Brunic Solimovic Regosol. In this soil, several light-yellow mottles occur. The upper soil (layer 6a, MIS 5a) is a pedosediment in most of the sections, turning into moderately developed soil in section #1 (Fig. 3C), where it includes the Ak@b and Bwk@b horizons. The soil is disturbed by solifluction, soil veins, and a reticulate post-cryogenic texture. The latter resulted in a platy structure. Thus, the soil is classified as a Calcaric Solimovic Regosol.

The Uday unit (layer 5, MIS 4) comprises loess and solifluction beds, both calcareous and silty. Carbonates are both secondary and primary with an explicit predominance of calcified root cells and soft nodules. In the lower part of the unit, there are horizontal laminae and inclusions of humified soil material. In the upper part, the loess is weakly altered by subsequent pedogenesis.

The Vytachiv unit (layer 4, MIS 3) is represented by brown soil with two distinct horizons—Agb and Bwb—therefore, it was attributed to a Gleyic Cambisol. The soil is calcareous with a predominance of secondary carbonates, including hard nodules up to 4 cm in diameter. The Cambisol is overlain by thin tundra gley (layer 4a).

The Bug unit (layer 3, MIS 2), similarly to the Uday unit, consists of loess and solifluction beds. The solifluction bed is dominated by brown soil material. The loess material here forms only thin interbeds. Soft carbonate nodules and calcified root cells dominate the solifluction bed, whereas dispersed powdery lime and pseudomycelia dominate the loess bed. Fractures in the loess open at different levels.

The Dofinivka unit (layer 2, MIS 2) is represented by a weak calcareous soil with explicit signs of gleying in the lower part. Unlike other paleosols, the Dofinivka soil bears no signs of mass-movement processes. The soil is classified as a Calcaric Gleyic Regosol. In sections #1 and #2, the Dofinivka unit is overlain by a loess unit disturbed by Holocene krotovinas. However, in section #3, within the loess unit, a Gleysol (layer 1b) affected by cryoturbation and ice-wedge pseudomorphs is present.

The Holocene soil is truncated owing to prolonged ploughing and erosion along the slope. The chernic horizon is relatively shallow (0.3 m), and carbonates are found below a depth of 0.3–0.4 m, showing a Bk horizon. This enables an interpretation of the Holocene soil as a Calcic Chernozem.

Micromorphology

The micromorphology indicates the synsedimentary character of the MIS 5 soils, as evidenced by rounded and subrounded sand grains and their relative sorting. In the Ctgb horizon of the Kaydaky soil (layer 8, MIS 5e), sand grains are well rounded, attesting to the sedimentary provenance of the bed. Moreover, the micromorphology of the Kaydaky soil is typical for Retisols (Table 2). In the Btg@b horizon, the microstructure is angular blocky, and numerous clay coatings with humus impurities appear in the voids (Fig. 4L). Sand grains penetrate the micromass through microlayers enriched with clay coatings (Fig. 4K). These microlayers are well porous and vertically oriented, demonstrating sand penetration through glossae, a feature of Retisols. The EBt@b horizon is characterized by a platy microstructure and bleached micromass (Fig. 4J), with fragments of an argic horizon. In the AE@b horizon, the micromass is characterized by a pronounced microzonality, as evidenced by the alternation of domains enriched in Fe oxides and humus punctuations (Fig. 4I). Here, typic carbonate nodules appear for the first time.

The lower Pryluky soil (layer 7, MIS 5c) is characterized by a weak granular microstructure (Fig. 4G). The micromass is enriched in brown humus and has no signs of a birefringence fabric. There are also thin Fe–Mn hypocoatings and Fe-oxide depletion hypocoatings. Sand grains are concentrated along the planes or form circular patterns (Fig. 4H). The Brunic Solimovic Regosol (layer 6b, MIS 5a) has a platy microstructure with pronounced brown humus punctuations (Fig. 4F). Here, the roundness of the sand grains increases, indicating intense sedimentation. The Calcaric Solimovic Regosol (layer 6a, MIS 5a) is characterized by an angular blocky microstructure in the Bwk@b horizon and a subangular blocky microstructure in the Ak@b horizon (Fig. 4B). Only secondary carbonates are found since they are associated with channels and chambers as developed calcite hypocoatings (Fig. 4C). Moreover, needle-fiber calcite also occurs in voids in the form of polycrystalline chains according to Verrecchia and Verrecchia (1994). Manganese infillings are frequent in the channels and chambers (Fig. 4A), whereas Fe–Mn hypocoatings are developed along the planes (Fig. 4D).

The Vytachiv soil (layer 4, MIS 3) has weakly separated angular blocky and granular aggregates with silt concentrations on the walls of granules. The latter is an indicator of soil redeposition (Kühn et al., 2018). Thin carbonate hypocoatings, secondarily covered with Fe oxides, appear in several channels, whereas in the micromass, geodic, typic, and concentric Fe–Mn nodules (Fig. 5J), as well as typic carbonate nodules (Fig. 5I), occur. The latter bear signs of fracturing, probably due to their redeposition. The humus punctuations are well expressed.

The Dofinivka soil (layer 2, MIS 2) is the least developed soil in terms of micromorphology. A weak platy (Fig. 5C), granular, and crumby (Fig. 5B) microstructure is characteristic of the Awkb horizon, whereas a better-developed granular and subangular blocky (with even single crumby aggregates) microstructure is present in the Bgkb horizon (Fig. 5D). The Bgkb horizon shows pronounced redoximorphic features, Fe-oxide depletion hypocoatings (Fig. 5E), and many carbonate rhizoliths. In the Awkb horizon, carbonates are represented by hypocoatings and small nodules.

The Uday (MIS 4) and Bug (MIS 2) loess units are characterized by many carbonate pedofeatures, including hypocoatings (Figs. 5F and K), rhizoliths (Fig. 5G), and typic nodules. The micromass is micritic and the microstructure is rather platy (Fig. 5L). Furthermore, granular aggregates appear in the Uday loess (MIS 4), and many channels occur in the Bug loess (MIS 2). In the Prychornomorya loess unit, carbonates are represented only by dispersed micrite (Fig. 5A).

Recent soil is characterized by dark brown humus and a spongy microstructure with soil fauna excrements. In the Ahp horizon, single silt-size crystals of secondary calcite occur, whereas in the Bk horizon, dispersed micrite and thin calcite hypocoatings appear.

Paleocryogenic features

At the Smykiv site, evidence of cryogenesis was found at different stratigraphic levels (Fig. 3). The Dnipro alluvium (layer 10, MIS 6) was affected by cryoturbation, loading structures with an amplitude of up to 0.5–0.6 m at the base of the section, as well as irregular waves and folds in the middle part of the alluvial unit. The

https://doi.org/10.1017/qua.2024.51 Published online by Cambridge University Press

Table 2. Micromorphology of the Smykiv stratigraphic units.

			Structure					Voids
Unit	MIS	Genetic horizon	Spongy/Crumby	Granular	Subangular blocky	Angular blocky	Platy	Overall porosity
0	1	Ahp	+++++	-	+	-	-	++
		Bk	+++++	-	-	-	-	+++
1	2	Ck	-	-	+++	+	-	++
2		Awkb	+	+	+++	-	+	+++
		Bgkb	++	+	+++	+	-	++
3		Ckb	-	-	+++	-	++	+++
4	3	Bwgb	-	++	++++	+	-	++
5	4	Ckgb	-	+	++	-	+++	++++
6a	5a	Ak@b	-	+	++++	-	-	++
		Bwk@b	-	+	+++	++	-	++
6b		Ab	-	+	++	-	+	+++
7	5c	Ah@b	+	++	+++	-	-	+++
8	5e	AE@b	-	+	+	-	-	+
		EBt@b	-	+	-	-	++	++++
		Btg@b	-	-	++++	-	-	++
		Ctgb	-	++	++	-	-	+++

			Types of voids					Secondary carbonates				
Unit	MIS	Genetic horizon	Compound packing pores	Channels	Chambers	Vugs	Planar voids	Sparite infillings	Rhizoliths	Micrite infillings	Hypocoatings	Nodules
0	1	Ahp	++++	++	+	+	+	-	-	-	-	-
		Bk	++++	++	+	+	-	-	-	-	+	+
1	2	Ck	+++	-	-	++	++	-	-	+	-	-
2		Awkb	+++	++	+	+	++	-	+	-	++	+
		Bgkb	++	++	+	++	+++	+	++	-	+	+++
3		Ckb	++	++	+	+	+++	-	++	-	+++	+
4	3	Bwgb	+++	+	-	++	++	-	-	-	+	+
5	4	Ckgb	++++	+	+	+	++	+	+	-	++++	+++
6a	5a	Ak@b	++	++	+	++	+++	-	-	-	++	+++
		Bwk@b	-	++	++	++	+++	-	-	-	++++	+
6b		Ab	++++	-	-	-	+	-	-	-	-	-
7	5c	Ah@b	+++	-	-	+	++	-	-	-	-	-
8	5e	AE@b	+	-	-	++	+	-	-	+	-	+
		EBt@b	++++	-	-	-	-	-	-	-	-	-
		Btg@b	+	-	-	+	++	-	-	-	-	-
		Ctgb	++++	-	+	-	+	-	-	-	-	-

			Clay minerals	b-fabric				Clay coatings
Unit	MIS	Genetic horizon	Abundance	Speckled	Striated	Porostriated	Granostriated	Abundance
0	1	Ahp	++	+	+	-	+	-
		Bk	+	+	+	-	-	-
1	2	Ck	+	+	+	-	+	-

(*Continued*)

https://doi.org/10.1017/qua.2024.51 Published online by Cambridge University Press

Table 2. (*Continued.*)

Unit	MIS	Genetic horizon	Clay minerals	b-fabric				Clay coatings
			Abundance	Speckled	Striated	Porostriated	Granostriated	Abundance
2		Awkb	+	+	+	-	-	-
		Bgkb	++	++	+	-	+	-
3		Ckb	+	+	-	-	-	-
4	3	Bwgb	+++	++	++	+	+	-
5	4	Ckgb	+	+	+	-	-	-
6a	5a	Ak@b	++	++	+	-	+	-
		Bwk@b	++	+	+	-	++	-
6b		Ab	+	+	-	-	-	-
7	5c	Ah@b	+	+	-	-	+	-
8	5e	AE@b	+	+	+	-	+	+
		EBt@b	+	+	-	-	-	++
		Btg@b	+++	++	+++	+	++	++++
		Ctgb	+	+	-	-	-	++

Unit	MIS	Genetic horizon	Redoximorphic features						Excrements	Organic matter		
			Dendritic Mn nodules	Typic and geodic Mn nodules	Mn infillings	Fe-Mn nodules	Fe-Mn hypocoatings	Fe-oxide depletion hypocoatings	Abundance	Dark humus pigment	Brown humus pigment	Brown humus punctuations
0	1	Ahp	+	-	+	+	-	-	+++	+++	-	-
		Bk	-	+	+	-	-	-	++	-	+++	-
1	2	Ck	-	+	-	-	+	-	-	-	-	+
2		Awkb	-	-	-	-	-	-	+	-	-	++
		Bgkb	+	-	-	-	-	+	++	-	-	+++
3		Ckb	+	-	++	-	-	-	-	-	-	+
4	3	Bwgb	-	-	-	+++	+	-	-	-	-	+++
5	4	Ckgb	+	++	-	-	-	-	-	-	-	+
6a	5a	Ak@b	+	+	++	+++	-	-	-	-	-	++
		Bwk@b	-	-	-	+	+++	+	-	-	-	++
6b		Ab	+	-	-	+	-	-	-	-	-	+++
7	5c	Ah@b	-	-	-	+	+	-	+	-	++	-
8	5e	AE@b	-	-	-	+	++	++	-	-	-	++
		EBt@b	+	-	-	-	-	-	-	-	-	-
		Btg@b	+	-	-	-	+	-	-	-	-	+
		Ctgb	-	++	-	+	+	-	-	-	-	+

The classification corresponds to Stoops (2003) and Stoops et al. (2018). The semi-quantitative micromorphological analysis is as follows: - = none; + = few; ++ = common; +++ = frequent; ++++ = dominant. The developed paleosols are highlighted in grey; weak soils are highlighted in light-grey.

latter is associated with irregular faults. From the top of layer 9, wedge-shaped soil veins open up to 1.0 m in depth.

The Kaydaky soil (MIS 5e) is disturbed by small wedge-shaped soil veins (up to 0.9 m in depth). The structures open from the top of the Btg@b horizon and are filled with material from there. Moreover, the Retisol is disturbed by reticulate post-cryogenic textures accentuated by iron oxides in the Btg@b horizon and lenticular post-cryogenic textures in the AE@b horizon. Layered post-cryogenic textures occur rarely.

The Pryluky soils (MIS 5a-c) are disturbed by two cryogenic levels. The lower level contains soil veins (up to 1.5 m in depth) filled with dark material of Phaeozem (layer 7) and bent by solifluction (up to 30–40°). Remarkably, only the lower (layer 7, MIS 5c) and upper (layer 6a, MIS 5a) Pryluky soils are deformed by solifluction, whereas the middle soil (layer 6b) remains undisturbed. This indicates the presence of two different solifluction layers, which is also confirmed by the existence of a network of narrow vertical soil veins (up to 0.9–1.1 m in depth) filled with

https://doi.org/10.1017/qua.2024.51 Published online by Cambridge University Press

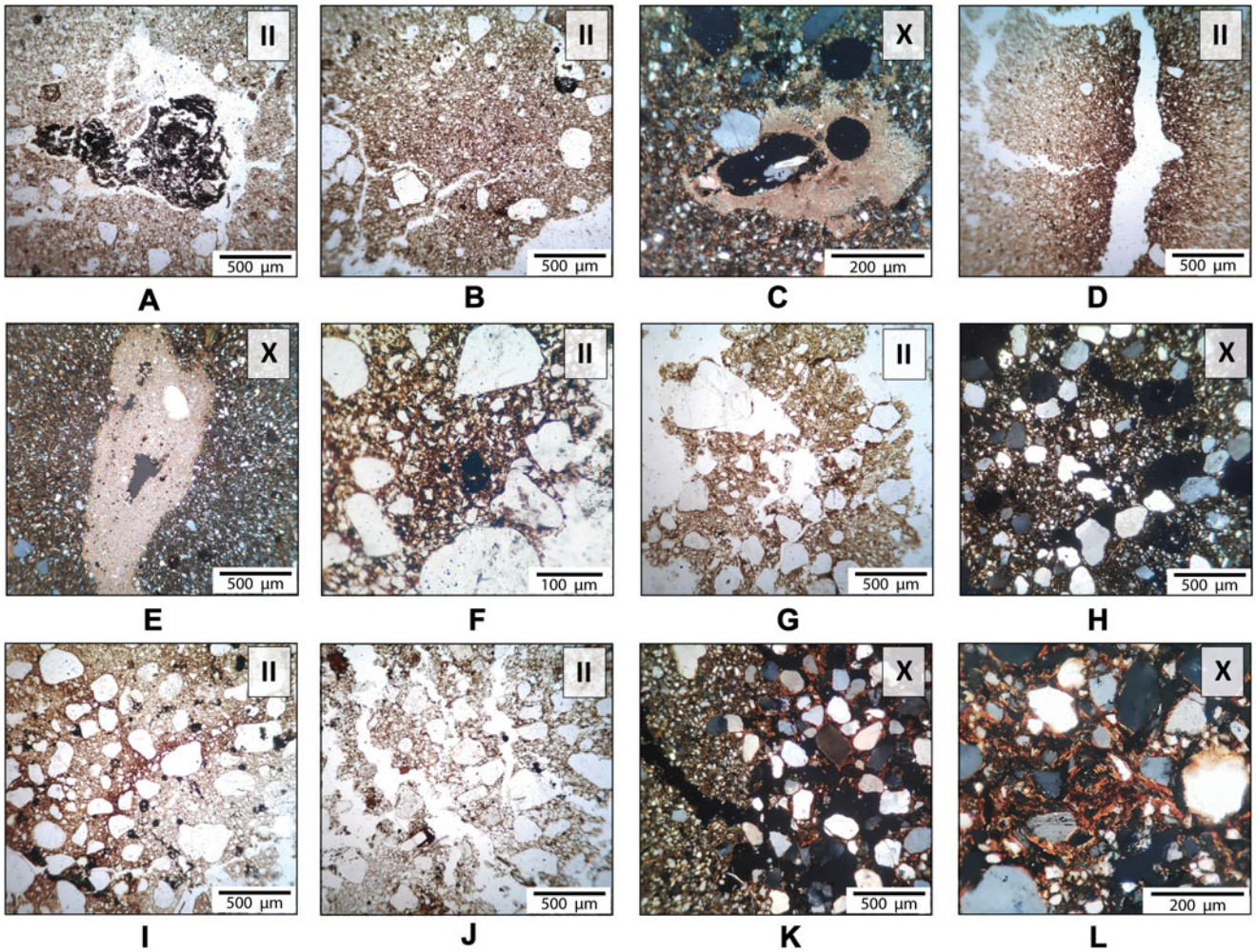

Figure. 4. Micromorphology of the Kaydaky and Pryluky soil units (MIS 5). (A) intrusive manganese nodule in chamber, Ab@b horizon, layer 6a; (B) brown humus punctuations; note sand concentration around a granular aggregate, Ak@b horizon, layer 6a; (C) calcite hypocoating in channel, Ak@b horizon, layer 6a; (D) Fe–Mn hypocoating along a plane, Bwk@b horizon, layer 6a; (E) geodic micritic nodule, Bwk@b horizon, layer 6a; (F) dark brown humus punctuations and small Fe–Mn nodule between sand grains, Ab horizon, layer 6b; (G) crumby aggregates between sand grains, Ah@b horizon, layer 7; (H) circular pattern of sand grains, Ah@b horizon, layer 7; (I) microzonal groundmass: bleached domains alternate with ferruginous, AE@b horizon, layer 8; (J) bleached groundmass and platy aggregates, EBt@b horizon, layer 8; (K) silty primary groundmass (on the left) penetrated by sandy glossae with clay coatings (on the right), Btg@b horizon, layer 8; (L) fibrous clay coatings in the soil matrix, Btg@b horizon, layer 8. II, plane polarized light; X, cross polarized light.

brown material from unit 6a. Moreover, an ice-wedge pseudomorph penetrates the Pryluky soil that is 1.8 m in depth and 1.0 m in width at the mouth. The ice-wedge pseudomorph is filled with loose calcareous pale-yellow loess. The upper part of the structure is slightly bent by solifluction and overlain by a streak of redeposited humified material.

The upper solifluction bed is connected to the Bug unit (layer 3, MIS 2), showing plastic deformation of the soil material interbedded with the loess. From the loess, thin frost fissures (up to 0.8 m in depth) open. In section #3, the upper 1.5 m of an ice-wedge pseudomorph filled with Gleysol was exposed. Thin frost fissures (up to 1 m in depth) are found in the overlying loess.

Grain-size composition and carbonate content

The grain-size composition of the MIS 5 soils (layers 6–8) differs from the upper horizons in the increased sand content (up to 40–60%) and, respectively, low median particle diameter (3.2–5.3 phi) and average particle radius (4.3–5.2 phi) values (Fig. 6). In the upper Pryluky soil (layer 6a, MIS 5a), the sand content decreases significantly (5–40%), showing peaks in the solifluction horizons and in the Prychornomorya loess (up to 16–30%). In contrast, the upper part of the section (layers 1–5) is characterized by a high content of coarse silt (50–70%), including in the recent soil (57–59%). The clay content is the highest (25–34%) in the Dofinivka soil (layer 2).

The calcium carbonate content gradually decreases down the section, showing peaks beneath the recent soil (layer 1) and in the Bug (layer 3) and Uday (layer 5) loesses. In the middle Pryluky soil (layer 6b) carbonates are not found (due to leaching); however, field observations have shown that occasional secondary carbonates are encountered down to the Kaydaky soil (layer 8).

Magnetic susceptibility

Low-frequency mass-specific magnetic susceptibility (χ_{lf}) reveals weak magnetic enhancement in the loess, paleosol, and aeolian sand samples, ranging between 7 and 20×10^{-8} m^3/kg, with a

https://doi.org/10.1017/qua.2024.51 Published online by Cambridge University Press

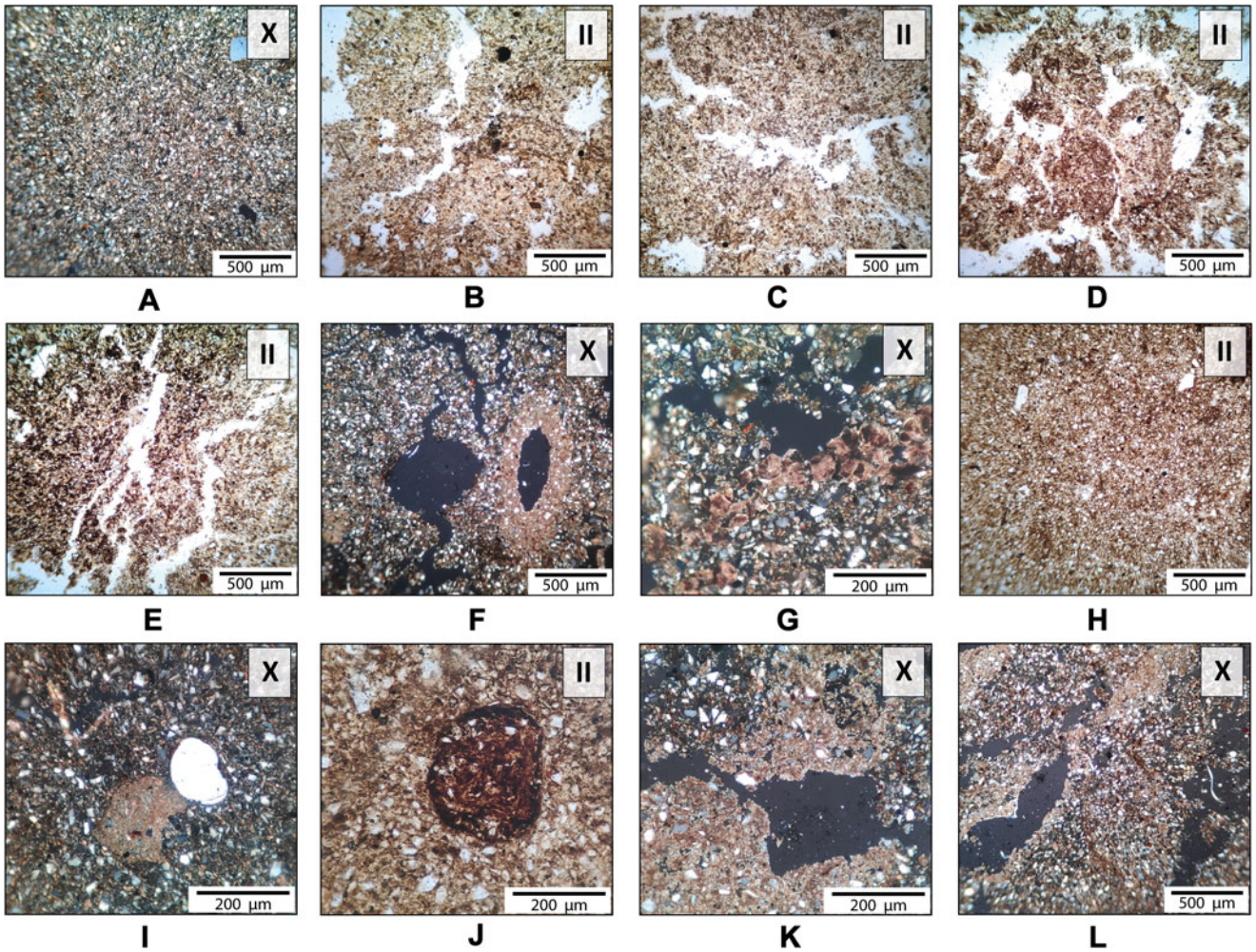

Figure 5. Micromorphology of layers 1–5. (A) loess micromass, Ck horizon, layer 1; (B) crumby microstructure, Awkb horizon, layer 2; (C) weak platy microstructure, Awkb horizon, layer 2; (D) granular aggregates, Bgkb horizon, layer 2; (E) groundmass microzonality by Fe compounds, Bgkb horizon, layer 2; (F) empty channel and channel with calcite hypocoating, Ckb horizon, layer 3; (G) calcified root cells in the loess matrix, Ckb horizon, layer 3; (H) pronounced humus punctuations, Bwg horizon, layer 4; (I) typic carbonate nodule and rounded sand grain, Bwg horizon, layer 4; (J) concentric Fe–Mn nodule, Bwg horizon, layer 4; (K) developed carbonate hypocoating, Ckg@b horizon, layer 5; (L) micritic micromass and carbonate hypocoatings along planes, Ckg@ horizon, layer 5. II, plane polarized light; X, cross polarized light.

median of 11.5×10^{-8} m^3/kg. This indicates a low total concentration of ferrimagnetic particles (Fig. 7). Only the Holocene soil reaches the maximum χ_{lf} values of up to 38×10^{-8} m^3/kg in its uppermost layer. Relatively high χ_{lf} values are characteristic of the uppermost part of the uppermost MIS 2 (Prychornomorya, pc) loess (up to 20×10^{-8} m^3/kg), interstadial soils of the MIS 2 (Dofinivka, df) unit (17×10^{-8} m^3/kg), and the MIS 5c (lower Pryluky, pl_{1b}) subunit (19×10^{-8} m^3/kg). The alternation of other loesses, paleosols, and pedosediments is not expressed in the magnetic susceptibility record (Fig. 7).

The variations of low-frequency (χ_{lf}) and frequency-dependent (χ_{fd}) susceptibilities show the same trend with depth, demonstrating significantly lower χ_{fd} values, with a median of 4.1×10^{-8} m^3/kg in the Holocene soil and 0.5×10^{-8} m^3/kg in the rest of the units (Fig. 7).

Percent frequency-dependent magnetic susceptibility ($\chi_{fd\%}$) is a direct measure of the contribution of superparamagnetic (SP) grains (Dearing et al., 1996). In general, $\chi_{fd\%}$ percentages greater than 6% indicate a considerable abundance of SP ferrimagnetic particles, while maximum observed values of ≥10–12% indicate that susceptibility is dominated by SP ferrimagnets, formed owing to pedogenic processes. Values of $\chi_{fd\%}$ of <5% are typical for samples in which stable single-domain grains dominate the assemblage or where extremely fine grains (<0.005 μm) dominate the SP fraction.

The plot of χ_{fd} versus χ_{lf} (Fig. 8A) reveals four closely clustered groups of samples: (1) the Holocene soil with the highest χ_{lf} and χ_{fd} values in the section; (2) the uppermost part of the Prychornomorya loess with relatively high χ_{lf} but low χ_{fd}; (3) other loess samples with very low χ_{lf} and χ_{fd} patterns; and (4) paleosol and pedosediment samples with relatively low χ_{lf} values but higher χ_{fd} values than those observed in groups (2) and (3). The plot of χ_{fd} versus $\chi_{fd\%}$ (Fig. 8B) indicates that most of the soil and pedosediment samples have $\chi_{fd\%}$ percentages >10%, in which SP grains dominate the assemblage, and thus $\chi_{fd\%}$ can be used quantitatively to estimate their total concentration (Fig. 8C).

At Smykiv, the MIS 5 (Pryluky–Kaydaky) paleosol series demonstrates a higher degree of pedogenesis (highest mean $\chi_{fd\%}$ values in the section up to 12–13%) compared to that in the younger interstadial paleosol units (only 3–3.5%) (Fig. 8C). Relatively

https://doi.org/10.1017/qua.2024.51 Published online by Cambridge University Press

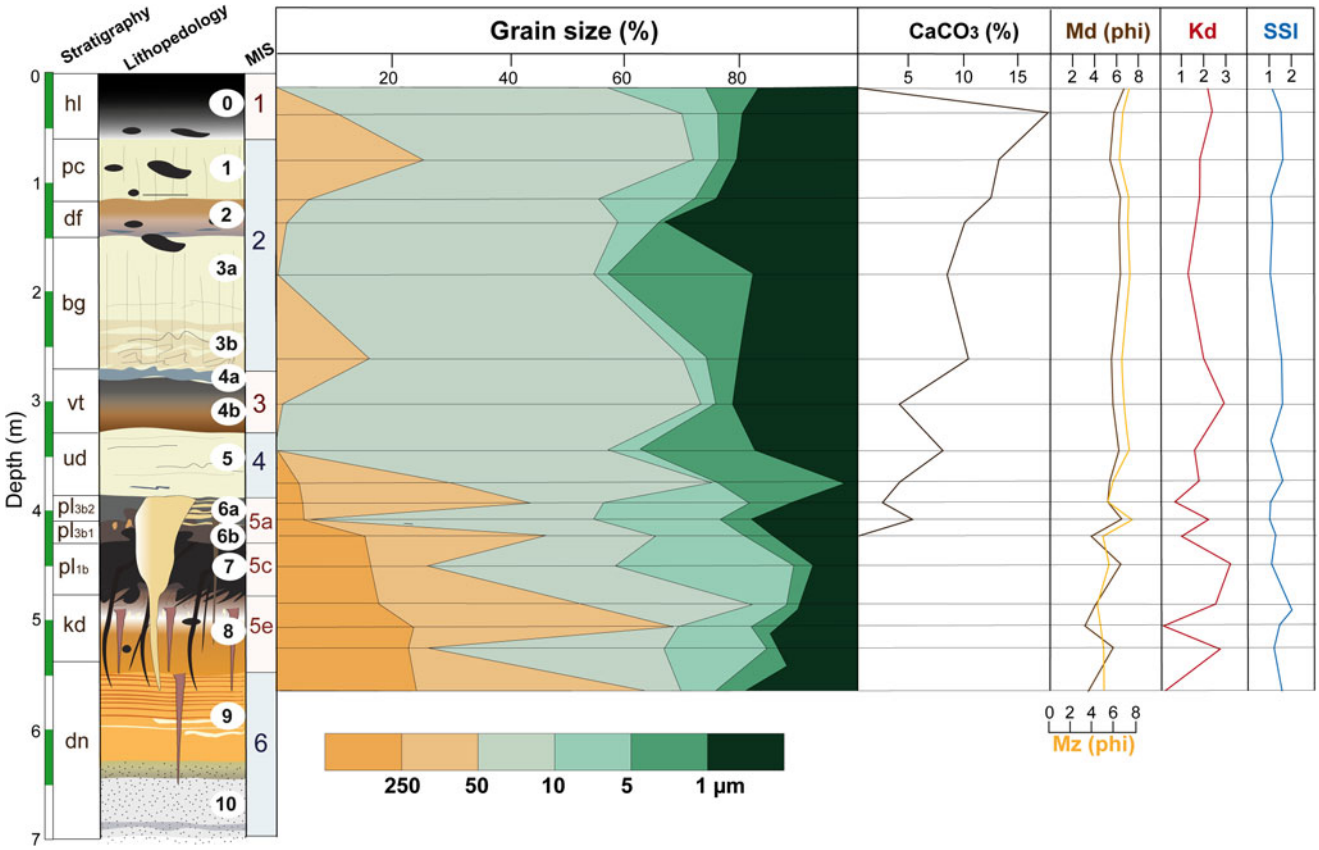

Figure 6. Grain-size data from the Smykiv site (explanation in the text). Md, median particle radius; Kd, loess index; SSI, soil/sedimentation index. See Table 1 for definition of stratigraphic units.

high $\chi_{fd\%}$ values (6%) are also observed in the upper MIS 2 (Prychornomorya) loess and pseudomorphs (due to reworking by the recent soil).

Other magnetic parameters

IRM acquisition curves for typical samples are displayed in Figure 8D. The curves reach ~90% of the IRM_{1T} when the applied field (H) is 300–350 mT for the majority of the paleosol and pedosediment samples, 400 mT for two loess samples, and 450 mT for one pedosediment sample from MIS 5a (upper Pryluky subunit, layer 6a). This behavior reveals the existence of "soft" magnetic minerals (magnetite and/or maghemite), especially in soils and pedosediments. However, the curves do not climb rapidly and the data indicate the presence of "hard" magnetic components (such as hematite), in particular, from loess and the youngest pedosediment layers. Nonetheless, a sample from the Holocene soil reaches 100% of the IRM in a field of 150 mT, which indicates the dominance of "soft" magnetic minerals (e.g., magnetite).

ARM (χ_{ARM}) and the ratios ARM/IRM_{1T} and χ_{ARM}/χ_{lf} are indicators of stable single-domain (SSD) particles (Maher, 1998; Evans and Heller, 2003; Liu et al., 2012) due to the fact that multidomain (MD) grains generally have exceedingly low coercivities and are unable to retain any significant ARM. ARM, similarly to frequency-dependent susceptibility, is particularly high for magnetite grains close to the SP/viscous boundary (see Maher, 1998). At Smykiv, values of ARM, ARM/IRM_{1T}, and χ_{ARM}/χ_{lf} increase in the entire MIS 5 pedocomplex (Fig. 7) and correlate with soil/loess boundaries more precisely than the magnetic susceptibility peaks (compare Fig. 7).

The IRM_{1T}/χ_{lf} ratio (Fig. 7) is a grain-size proxy in dominantly magnetite-bearing sediments (Liu et al., 2012); however, the IRM_{1T}/χ_{lf} seems distorted due to the significant contribution of hematite according to the IRM acquisition curves (Fig. 8A) and S and HIRM indices (Fig. 7). The S ratio is a common parameter that is used to quantify the proportion of "hard" and "soft" magnetic minerals (Evans and Heller, 2003). The S ratio is expressed as the ratio of an IRM acquired at some non-saturating backfield (often −300 mT) measured after the acquisition of the saturation IRM (SIRM). Values close to unity indicate that the remanence is dominated by "soft" ferrimagnets. The remanence held by "hard" magnetic minerals within sediments is estimated by the "hard" IRM or HIRM. HIRM is typically defined as the difference between the SIRM and backfield IRM_{-300mT} divided by 2.

The S ratio in the Smykiv section weakly depends on the lithology, but samples can be divided into two groups (Fig. 7). The S ratio of less than one-third of specimens (in particular, from the Pryluky soil) is close to 1, indicating a total dominance of magnetite, whereas the S ratio of more than two-thirds of samples (primarily, loess) fluctuates in the range between 0.8 and 0.9, suggesting a higher contribution of hematite. Since the HIRM increases with the increasing fraction of magnetically "hard" minerals, the S ratio is negatively correlated with the HIRM (Fig. 7).

https://doi.org/10.1017/qua.2024.51 Published online by Cambridge University Press

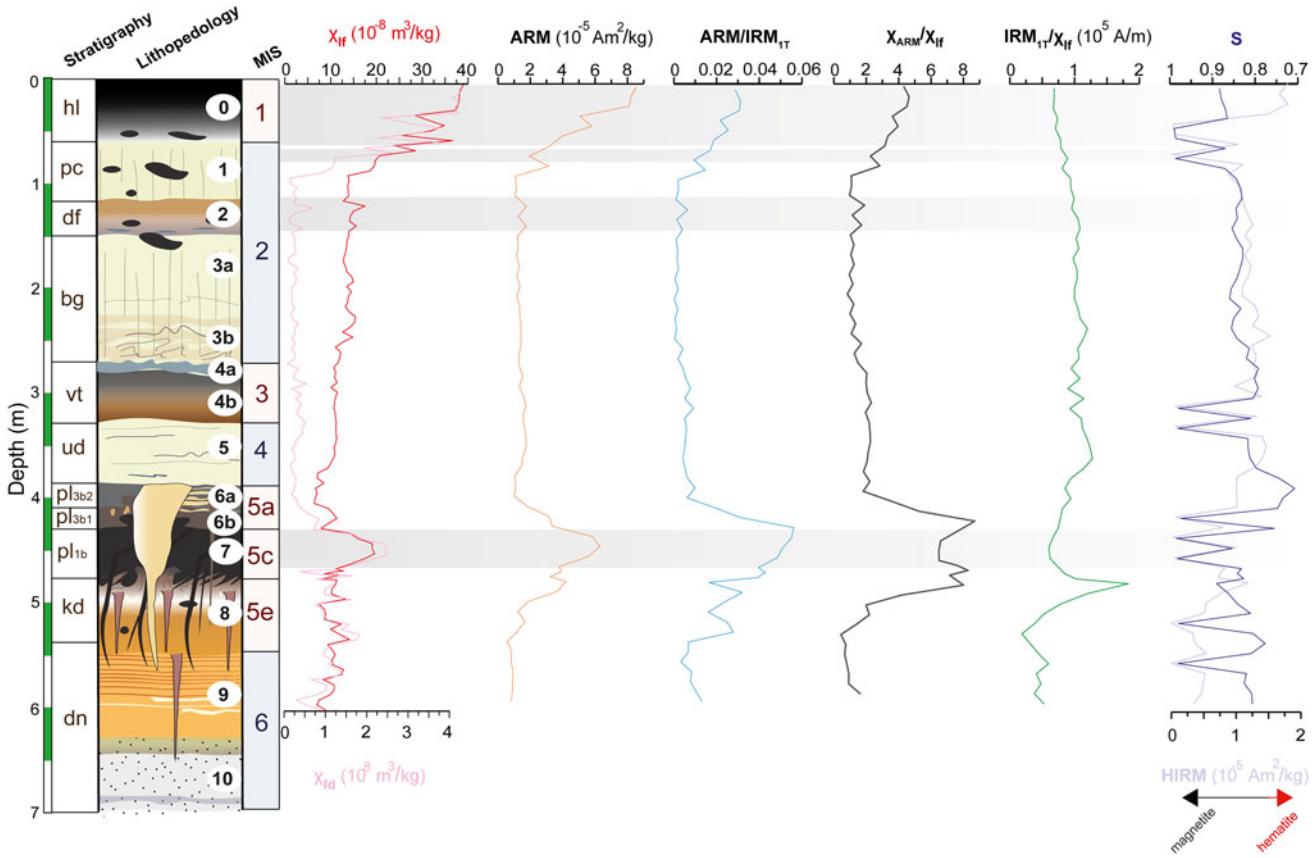

Figure 7. Variations of selected rock magnetic parameters along lithologic column of the Smykiv section (explanation in the text). See Table 1 for definition of stratigraphic units.

Discussion

Chronostratigraphic attribution

The Smykiv sequence correlates with the Upper Pleistocene Kolodezhi and Novyi Tik sections (Bonchkovskyi, 2020a), Korshiv (Fedorowicz et al., 2013) and Boyanychi (Kusiak et al., 2012) sections in northwestern Ukraine, as well as with the Vyazivok sequence in central Ukraine (Veklych et al., 1984; Rousseau et al., 2001; Haesaerts et al., 2016; Hlavatskyi and Bakhmutov, 2020) (Figs. 9 and 10, Table 3). The Smykiv site has not yet been dated, therefore the correlation is based on pedogenic, magnetic, and cryogenic features. In Figure 11, the Smykiv section is correlated with the local stratigraphic scheme of western Ukraine (Bogucki, 1986; Bogucki et al., 2014) and the regional Quaternary stratigraphic framework by Veklych et al. (1993) modified by Gerasimenko (2004), Gozhik et al. (2000, 2014), and Matviishyna et al. (2010).

At the Smykiv site, layers 6–8 form a recognizable pedocomplex, which is the first pedocomplex from the surface in western Ukraine and is assigned to the Horokhiv soil unit in the local loess stratigraphic scheme (Bogucki, 1986; Łanczont and Boguckyj, 2007; Fedorowicz et al., 2013). In the most complete sections, the Horokhiv unit comprises a lower (Eemian) soil with a developed Bt horizon and up to three humified interstadial (MIS 5a and 5c) soils (Kolodiiv soils) (Łanczont et al., 2022). A similar soil succession was recorded at the Smykiv site, where three humified soils are superimposed on a Retisol. In the nearby Novyi Tik sequence, these soils are separated by sand beds with cryogenic features (mostly solifluction and soil veins), indicating the stadial periods of MIS 5b and 5d (Bonchkovskyi, 2020a). At the Novyi Tik site, the lower forest soil (Retisol and Luvisol) bears signs of an Eemian pollen succession, which proves the correlation of Pedocomplex I with MIS 5. At the Smykiv site, non-soil deposit beds between the soils of the first pedocomplex are absent; however, cryogenic features reliably indicate cold stages and pedogenesis interruption. At least two cryogenic levels can be distinguished that appear to correlate with MIS 5b and 5d.

In central Ukraine, the bipartite pedocomplex of MIS 5, consisting of lower forest and upper humified soils, is designated as the Kaydaky and Pryluky units, respectively (Rousseau et al., 2001; Vozgrin, 2001; Gerasimenko, 2006, 2010a; Matviishyna et al., 2010; Haesaerts et al., 2016; Hlavatskyi and Bakhmutov, 2020). The lower forest soil in the LPSs of the Kyiv loess region (Stari Bezradychi, Pyrogovo, and Muzychi sites) and the Dnipro Lowland (Vyazivok; Fig. 10) directly overlies the Dnipro till, which has previously been suggested to be of MIS 8 age (Veklych et al., 1993; Łanczont and Boguckyj, 2007; Gozhik et al., 2012, 2014). It was widely accepted that the Dnipro (Dnieper) glaciation is the equivalent of the Odradian glaciation in Poland (Lindner et al., 2006). Recent studies demonstrate that the Odradian glaciation occurred during MIS 6 (Marks, 2023), as was previously concluded for the Dnipro glaciation in Ukraine (Rousseau et al., 2001; Vozgrin, 2001; Gerasimenko, 2010b; Matoshko, 2011). Palynological studies have revealed the Eemian pollen succession in the soil directly overlying the Dnipro till, attributed to the Kaydaky soil unit (Gerasimenko,

https://doi.org/10.1017/qua.2024.51 Published online by Cambridge University Press

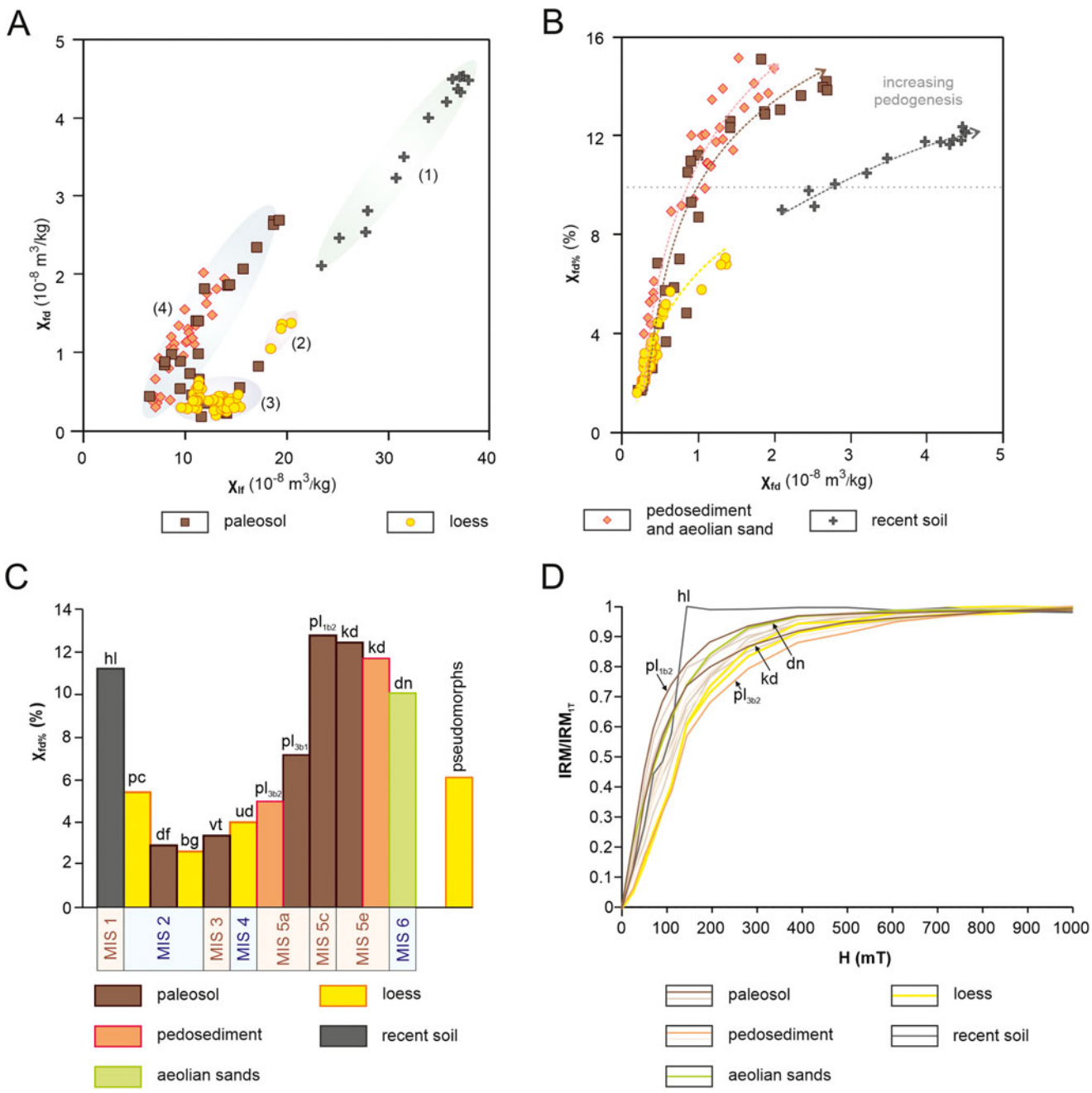

Figure 8. (A) Frequency-dependent susceptibility (χ_{fd}) plotted against low-frequency susceptibility (χ_{lf}) and (B) percentage frequency-dependent factor ($\chi_{lf\%}$) plotted against frequency-dependent susceptibility of main lithologic groups of samples from the Smykiv section. (C) Mean $\chi_{lf\%}$ values of each stratigraphic unit of the Smykiv section. (D) Examples of isothermal remanent magnetization acquisition curves of typical samples. Selected clusters of values (A) are shaded by different colors (see text for explanation). Note that χ_{fd} and $\chi_{fd\%}$ both increase with enhanced pedogenesis. Abbreviations: hl, Holocene; pc, Prychornomorya; df, Dofinivka; bg, Bug; vt, Vytachiv; ud, Uday; pl_{3b1}, Upper Pryluky; pl_{3b2}, Lower Pryluky; kd, Kaydaky; dn, Dnipro.

2006). Therefore, it was proposed to correlate the Kaydaky unit with MIS 5e and the Pryluky unit with MIS 5a–c (Gerasimenko, 2006; Gerasimenko and Rousseau, 2008). Nevertheless, other correlation schemes, in which the Dnipro unit corresponds to MIS 8 and the Kaydaky unit to MIS 7, are still being developed (Komar et al., 2018; Łanczont et al., 2023).

Taking into account that the Retisol (layer 8) in the Smykiv section is the first soil from the surface with a developed Bt horizon, it corresponds to the Kaydaky unit (MIS 5e). Consequently, the three humified soils (layers 6–7) correlate with the Pryluky unit (MIS 5a–5c) as they represent the first from the surface Chernozem-like soils. The two upper soils (layer 6) are designated as pl_{3b1} and pl_{3b2}, whereas the Phaeozem (layer 7) is designated as pl_{1b}.

The Gleyic Cambisol (layer 4) is designated as the Vytachiv unit, which is the equivalent of the Dubno unit in western Ukraine. The Calcaric Gleyic Regosol (layer 2) in the Smykiv section is attributed to the Dofinivka unit, whereas the underlying loess is attributed to the Bug unit and overlying loess to the Prychornomorya unit, all correlated with MIS 2. In the LPSs of western Ukraine and Poland, there are two Gleysols within the Upper Pleniglacial loesses (Bogucki, 1986; Jary and Ciszek,

https://doi.org/10.1017/qua.2024.51 Published online by Cambridge University Press

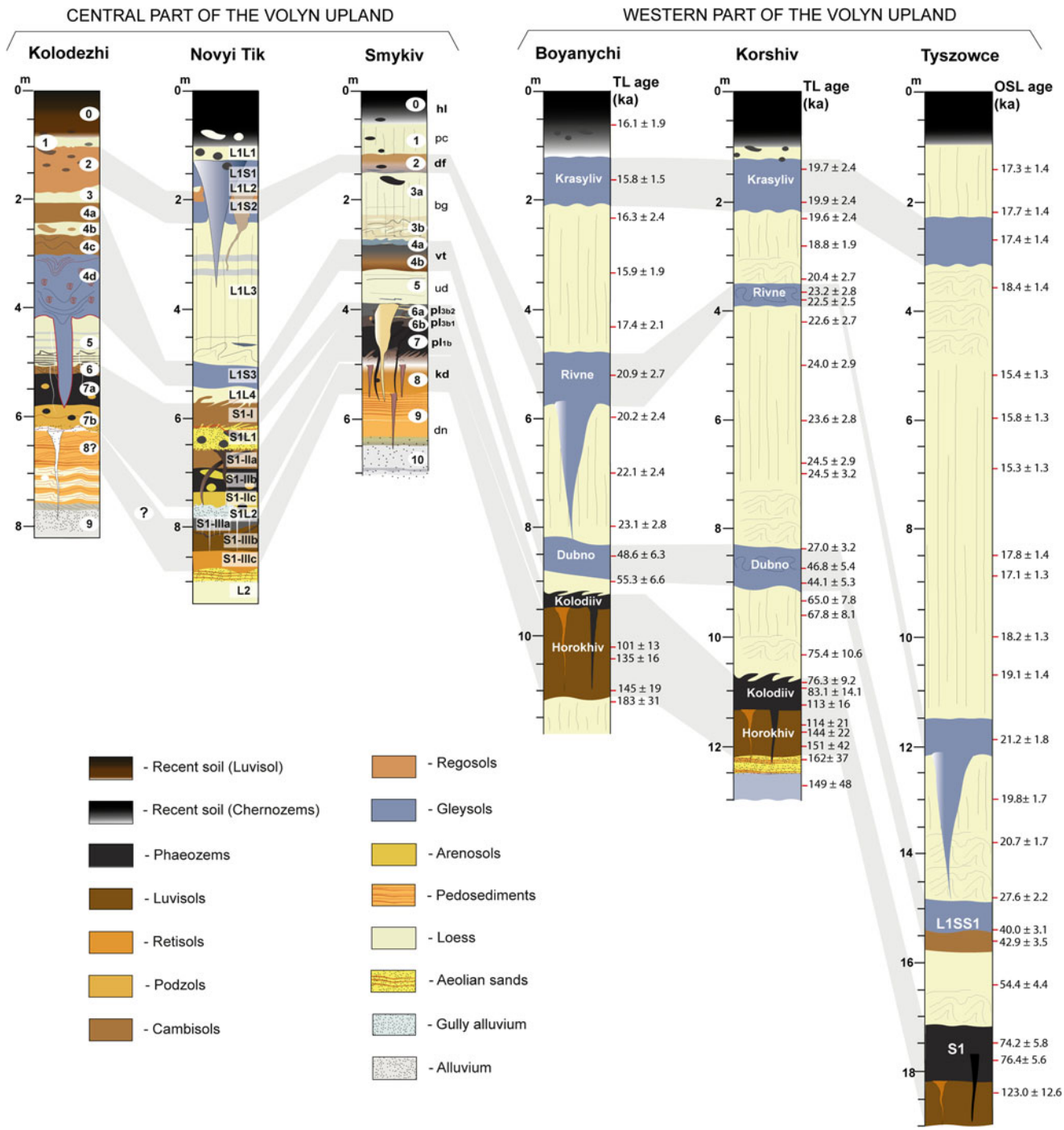

Figure 9. Correlation of the Smykiv section with key loess-paleosol sections of the Volyn Upland. Thermoluminescence (TL) dating results for the Korshiv section were obtained by Fedorowicz et al. (2013), and for the Boyanychi section by Kusiak et al. (2012); optically stimulated luminescence (OSL) dating results (45–63 μm) for the Tyszowce section were obtained by Moska et al. (2017).

2013; Fedorowicz et al., 2018), which correspond to the Rivne and Krasyliv units, both associated with levels heavily affected by cryogenesis. Many authors have assumed that the Dofinivka unit correlates with the Rivne unit, and the Krasyliv unit with the intra-Prychornomorya subunit (Łanczont and Boguckyj, 2007; Matviishyna et al., 2010; Bogucki et al., 2012), since they are the two youngest soils in the Pleistocene. Given the numerous dates for the Rivne and Krasyliv units in western Ukraine and the Dofinivka unit in central Ukraine, the question of correlation of these stratigraphic units is quite problematic (Jary and Ciszek, 2013; Dzierżek et al., 2022). Numerous dates for the Dofinivka unit in the LPSs of eastern and southern Ukraine range between 15 and 19 ka (Gerasimenko, 1997, 2004, 2011), which correspond to the dates for the Krasyliv unit in western Ukraine (Kusiak et al., 2012; Fedorowicz et al., 2013, 2018) but not the Rivne unit, which seems to be older and is dated mainly to 19–23 ka (Kusiak et al., 2012; Fedorowicz et al., 2013; Łanczont and Madeyska, 2015). Furthermore, the Rivne soil unit is significantly better developed

https://doi.org/10.1017/qua.2024.51 Published online by Cambridge University Press

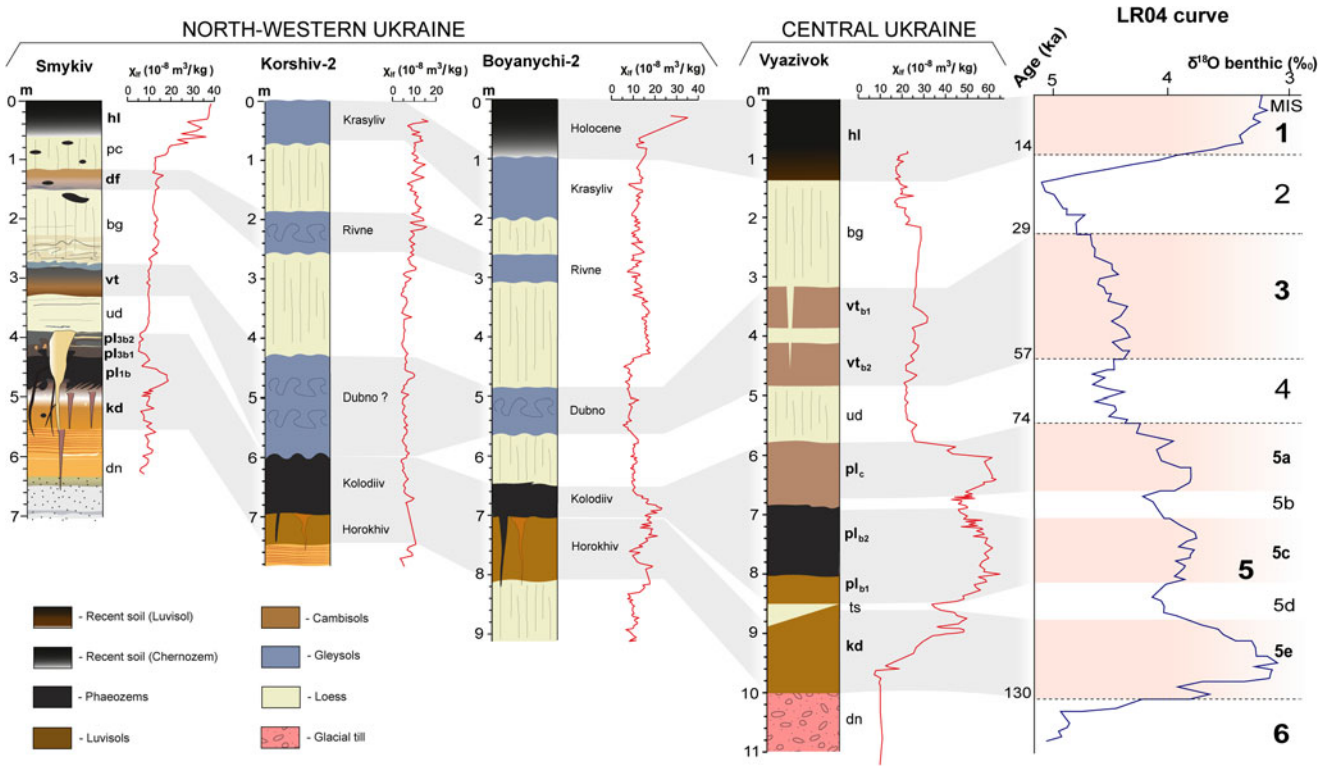

Figure 10. Correlation of the Smykiv section with the nearby Korshiv and Boyanychi loess sections in the Volyn Upland, Vyazivok section in the Dnipro Lowland (central Ukraine), and the stacked marine isotope LR04 curve (adapted from Lisiecki and Raymo, 2005). Magnetic susceptibility data have been adapted for the Korshiv and Boyanychi sections from Hlavatskyi et al. (2016), and for the Vyazivok section from Hlavatskyi and Bakhmutov (2020).

than the Krasyliv unit. The latter is often represented by gleyed loess beds. In western Europe, relatively developed soils in the upper part of the Weichselian loess are dated to 20–23 ka (Guiter et al., 2003; Haesaerts et al., 2003; Antoine et al., 2016), which corresponds to obtained ages for the Rivne unit. Taking into account the numerous dates from the LPSs of western Ukraine, provided by Kusiak et al. (2012), Fedorowicz et al. (2013, 2018), and Łanczont and Madeyska (2015), it can be assumed that both the Rivne and Krasyliv units correspond to the Dofinivka unit in central Ukraine, and the status of the Dofinivka unit in the Quaternary stratigraphic framework of Ukraine should be reconsidered. It can be tentatively assumed that the Rivne unit corresponds to the Lower Dofinivka subunit (df_1) and the Krasyliv unit to the Upper Dofinivka subunit (df_3). Thus, layer 2 in the Smykiv section correlates with the Rivne unit, whereas layer 1b (Gleysol in excavation #3) is attributed to the Krasyliv unit.

In terms of stratigraphic nomenclature for the Chinese and Danubian loesses (Liu, 1985; Kukla and An, 1989; Jordanova and Peterson, 1999; Marković et al., 2015), adapted by Łanczont et al. (2022) for western Ukraine and Poland, the Dnipro unit at Smykiv corresponds to the L2 unit, the Kaydaky–Pryluky pedocomplex to the S1 unit, and the Uday–Prychornomorya loess to the L1 unit (Fig. 11).

Pedogenesis and sedimentary environment

Compared to other LPSs in northwestern Ukraine, the Smykiv loess-paleosol sequence is characterized by thinner loess units and well-developed soils, namely a well-developed pedocomplex of MIS 5, moderately developed soil of MIS 3, and weakly developed soil of MIS 2. The MIS 5 soils bear signs of a synsedimentary origin, which is a characteristic of many LPSs in the southern and central parts of the Volyn Upland (Bonchkovskyi et al., 2023b). The coarse texture of MIS 5 soils can be explained by the contribution of aeolian sand to the pedogenesis, or the soils (especially those of MIS 5e) could inherit their texture from the parent material represented by aeolian sands. The pedogenesis was presumably interrupted by cold events as evidenced by cryogenic features, when erosion activated leading to soil truncation.

The Kaydaky soil (MIS 5e) meets the criteria of an Albic Glossic Retisol as evidenced by pronounced albeluvic glossae and abrupt textural differences. In the Btg@b horizon, there are many clay coatings with humus impurities. Sand intrusions into loamy material of an argic horizon at the microscale are another indicator of retic properties. Intrusions are enriched in clay coatings as a result of facilitated illuviation in coarse sediments. On the other hand, sand concentrations in inter-pedal voids are considered to be a result of repetitive freeze-thaw cycles in boreal soils (Van Vliet-Lanoë and Fox, 2018). Seasonal freezing also led to a platy structure of the EBt@b horizon and was seen both at the macro- and microscale. Despite the contemporary spread of Retisols under boreal mixed forests, we consider that retic properties are manifested owing to coarse-grained parent material, as was reported at the Novyi Tik site, where Retisols were formed on sands and Luvisols were formed on loess (Bonchkovskyi, 2020a).

Features of deep seasonal freezing in the Retisol seem to have occurred during the late phase of soil formation. Furthermore, wedge-shaped structures open from the top of the Btg@b horizon.

https://doi.org/10.1017/qua.2024.51 Published online by Cambridge University Press

Table 3. Common features of the marker stratigraphic units of the Smykiv sequence and dated sites at Korshiv (after Fedorowicz et al., 2013) and Boyanychi (after Kusiak et al., 2012).

			Korshiv		Boyanychi		
Common feature	Lithopedology	Smykiv	Unit	Dating	Unit	Dating	MIS
Upper Gleysol associated with the largest ice-wedge pseudomorphs	Gleysol	Unit 1b (excavation #3) (Upper Dofinivka)	Krasyliv (2e)	19.7–19.9 ka	Krasyliv (2e)	15.8 ka	2
Better developed Gleysol, occasionally affected by solifluction or smaller ice-wedge pseudomorphs	Gleysol, rarely with an incipient Bw horizon	Unit 2 (Lower Dofinivka)	Rivne (2c)	22.5–23.2 ka	Rivne (2c)	20.9 ka	
Most developed loess horizon, comprising a well-developed solifluction horizon in the lower part	Loess	Unit 3 (Bug)	Loess (2a, 2b)	22.6–24.5 ka	Loess (2a, b)	22.1–23.1 ka	
Most developed Gleysol, in places of bipartite structure with a Bw horizon. Generally affected by solifluction or cryoturbation	Gleysol, in places with Bw horizon	Unit 4 (Vytachiv)	Dubno	27.0–46.8 ka	Dubno	48.6–55.3 ka	3
Second loess horizon, heavily disturbed by solifluction in the lower part and with ice-wedge pseudomorphs	Loess	Unit 5 (Uday)	Loess (4)	65.0–75.4 ka	Loess (4)	-	4
First from the surface well-developed humified soil disturbed by solifluction and soil veins. Tripartite in places	Phaeozems/ thin humified soils	Units 6–7 (Pryluky)	Kolodiiv (Upper Horokhiv)	76.3–113 ka	Kolodiiv (Upper Horokhiv)	-	5a–5c
First interglacial soil with a developed Bt horizon	Luvisol	Unit 8 (Kaydaky)	Lower Horokhiv	114–151 ka	Lower Horokhiv	101–145 ka	5e

These structures could have been formed under a cool climate, presumably during the Herning stade (MIS 5d). Given this, the soil continued to form during the Amersfoort interstade (MIS 5c). Many authors reported that soils with textural differences were not formed during interstadial periods (Łanczont and Boguckyj, 2007; Łanczont et al., 2015); however, there are studies corroborating Bt or Bth horizon formation in the first half of MIS 5c (Gerasimenko, 2006; Antoine et al., 2016; Haesaerts et al., 2016; Bonchkovskyi, 2019, 2020a). For instance, at the Novyi Tik site, the Podzol was formed on sands and the Luvisol was formed on loams (Bonchkovskyi et al., 2023b). Thus, it can be assumed that the Retisol at the Smykiv site continued to form during the Amersfoort interstade (MIS 5c), interrupted by a stage of climate deterioration during MIS 5d.

The MIS 5c soil (pl_{1b}) is disturbed by solifluction and soil veins, associated with cryogenic events (MIS 5b) between phases of pedogenesis. Owing to a relatively well-developed A horizon and primarily carbonate leaching, the pl_{1b} soil is classified as a Haplic Phaeozem. Domains with a crumby microstructure testify to significant biogenic activity. The soil has a synsedimentary origin as evidenced by a weak granular microstructure and elevated sand content. Furthermore, the soil underwent subsequent solifluction movement that probably led to the circular sand grain concentration pattern. However, it can also be caused by cryogenic sorting (Konishchev and Rogov, 1977), or solifluction and cryogenic sorting could manifest simultaneously (Van Vliet-Lanoë and Fox, 2018).

The soils of MIS 5a (pl_3) are less developed. The lower soil (pl_{3b1}, layer 6b) is thin and therefore classified as a Brunic Solimovic Regosol. Rounded sand grains appear in the soil identifying high sedimentation rates, which should lead to fast soil accretion. The micromass and organic matter of this soil considerably differ from those of the Phaeozem, which does not indicate the development of this unit as a pedosediment of underlying soil. In return, a sharp upper boundary and abrupt decrease in sand content upwards confirm soil truncation. Presumably, the soil pl_{3b1} (layer 6b) was primarily formed as a Cambisol similar to that of soil pl_{3b1} in central Ukraine (Gerasimenko, 2006; Haesaerts et al., 2016).

The upper MIS 5a soil (pl_{3b2}, layer 6a) is distinguished by a noticeable decrease in sand content and appearance of a blocky microstructure. The soil is weakly developed and turns into pedosediment downslope. The soil is the most calcareous among the MIS 5 soils, including needle-fiber calcite considered as secondary, formed owing to rapid evaporation of soil solutions saturated with calcite (Verrecchia and Verrecchia, 1994). It appears to be that the calcic horizon (numerous rhizoliths and soft nodules), superimposed on the two lower Pryluky soils, is related to the upper Pryluky soil, indicating steppe pedogenesis. In contrast to older soils of MIS 5, these ones presumably are not synsedimentary, or sedimentary contribution was decreased. A decreasing sand sedimentation rate is a feature of the LPSs in the southern part of the Volyn Upland (Bonchkovskyi et al., 2023b), where sands were considered primarily to be aeolian and/or colluvial.

https://doi.org/10.1017/qua.2024.51 Published online by Cambridge University Press

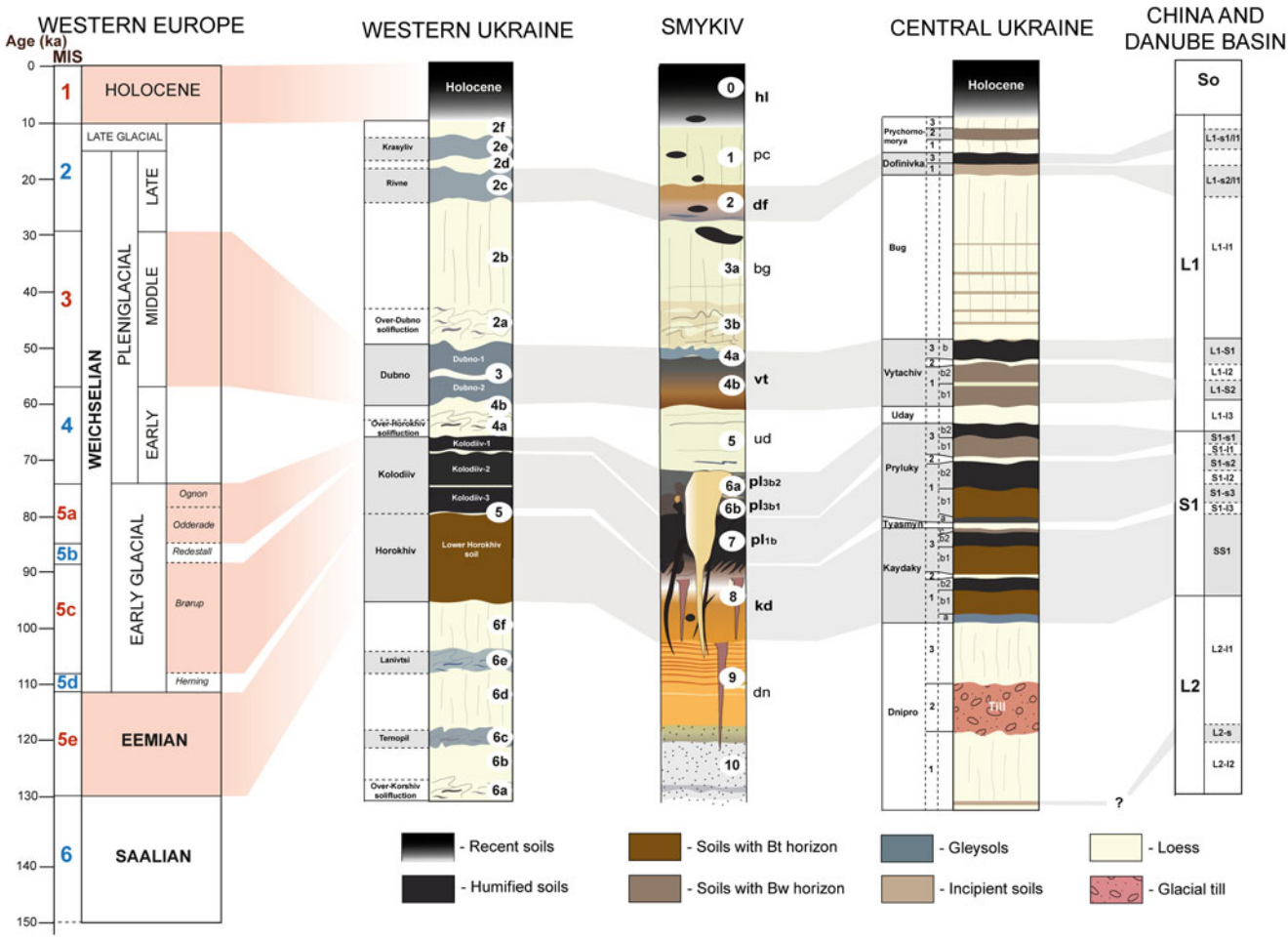

Figure 11. Correlation of the Smykiv section with the stratigraphic schemes of western Europe (Frechen et al., 2001; Guiter et al., 2003), western Ukraine (Bogucki, 1986; Łanczont and Boguckyj, 2007), central Ukraine (Veklych et al., 1993 modified by Gerasimenko, 2004; Matviishyna et al., 2010), and Chinese and Danubian stratigraphic models (Liu, 1985; Kukla and An, 1989; Jordanova and Peterson, 1999; Marković et al., 2015) adapted by Łanczont et al. (2022) for western Ukraine and Poland. The correlation proposed by Łanczont and Boguckyj (2007) is marked in red; the correlation proposed in this paper is marked in grey.

The almost complete disappearance of sand and the high loess index (Kd) values in the Pleniglacial units, both in the loess and in the soil units, indicate that sedimentary conditions in this region changed dramatically at the beginning of MIS 4 and aeolian silt accumulation predominated until the Holocene.

The Vytachiv soil (MIS 3) incudes recognizable Agb and Bwb horizons intrinsic for Gleyic Cambisol. A calcic horizon (pronounced pseudomycelia and cracks infilled with carbonates), superimposed on the Vytachiv soil, is probably related to the tundra gley (layer 4a) or can be attributed to the overlying solifluction bed enriched in brown soil material, which can be another soil, subsequently entirely redeposited by solifluction.

At the nearby Kolodezhi and Kovban sites, where the Dubno unit (MIS 3) is represented by a set of three soils, only the lower soil is classified as Gleysol, whereas the two upper soils are classified as Cambisols or Regosols. The same pattern was identified for the Vytachiv unit in the Kyiv loess region (Gerasimenko and Rousseau, 2008). Given the abrupt environmental changes in Europe during MIS 3 (Rasmussen et al., 2014), it can be assumed that Cambisols can represent particular interstadials in the study area, presumably the warmest ones.

The Dofinivka soil (MIS 2) is a weakly developed pale brown soil, which is tentatively classified as a Calcaric Gleyic Regosol. The soil cannot be classified as a Cambisol due to the absence of the Bw horizon. The soil was presumably formed in two phases. A better-developed microstructure and more-pronounced humus punctuations indicate more intense pedogenesis in the early phase. However, this occurred under seasonal waterlogging, which is marked by abundant redoximorphic features. In the second phase, the soil was formed in dry conditions, contributing to the secondary calcium accumulation and weathering processes. The Rivne (Lower Dofinivka) unit in the LPSs of western Ukraine is represented by a Gleysol (Bogucki, 1986; Fedorowicz et al., 2018). Cambic features appear at this level only in the Novyi Tik sequence (Bonchkovskyi, 2020a), which, though, disappear in the paleodepression (Bonchkovskyi et al., 2023a). At the Smykiv site, the brown color of the soil reveals an incipient cambic horizon, which does not meet the criteria of Cambisols.

The Upper Dofinivka (Krasyliv) soil is associated with ice-wedge pseudomorphs and can be attributed to a Cryosol/Gleysol, which is typical for LPSs of western Ukraine (Bogucki, 1986; Łanczont and Madeyska, 2015).

At the Smykiv site, loess units are characterized by distinct redoximorphic features, which indicates that they were formed

https://doi.org/10.1017/qua.2024.51 Published online by Cambridge University Press

in relatively humid conditions or areas with generally poor drainage. Widespread solifluction and plastic deformation in the lower parts of the loess horizons demonstrate wet conditions, primarily in the first half of the stadial periods. These make the loess characteristics at the Smykiv site similar to those of the central European loess subdomain of the northern European loess belt defined by Lehmkuhl et al. (2021). The well-developed periglacial phenomena and magnetic susceptibility patterns (discussed below) enhance this assumption. Taking into account similar features of the LPSs in many sites of western Ukraine (Bogucki, 1986; Bogutskiy et al., 2000; Nawrocki et al., 2006, 2007; Łanczont and Boguckyj, 2007; Jary, 2009; Łanczont et al., 2009, 2015, 2022, 2023; Kusiak et al., 2012; Fedorowicz et al., 2013, 2018; Jary and Ciszek, 2013; Bonchkovskyi, 2020a, 2020b; Bonchkovskyi et al., 2023a, 2023b), we propose delineating the eastern boundary of the central European loess subdomain through the central part of the Podillia Upland (see Fig. 1).

Cryogenesis

At the Smykiv site, cryogenic features are revealed at different levels and are represented by the following forms: ice-wedge pseudomorphs, soil veins and frost fissures, solifluction, and cryoturbation. At the Smykiv site, ice-wedge pseudomorphs are associated with the Krasyliv (Upper Dofinivka) unit (second part of MIS 2) and the Uday loess (MIS 4). An older ice-wedge pseudomorph is filled with calcareous loess and is bent by solifluction. The topography of the Vytachiv soil (MIS 3) is not related to the ice-body degradation, which points to ice-wedge degradation prior to the MIS 3. The younger ice-wedge pseudomorph at the Smykiv site is associated with the Krasyliv (Upper Dofinivka) gley unit, formerly designated as a buried active layer (Bogucki, 1986). Ice-wedge pseudomorphs of this level are the largest in LPSs of western Ukraine and Poland (Nechaev, 1983; Bogucki, 1986; Dolecki, 2003; Fedorowicz et al., 2018; Bonchkovskyi, 2020a). Recently, the upper part of the infillings of the ice-wedge pseudomorph at the Volochysk site (Podillia Upland) has been dated to 13.9–16.1 ka and correlated with the Heinrich event H1 (Fedorowicz et al., 2018). In Poland, multiple dates from ice-wedge pseudomorphs appear somewhat older: 20–29.5 ka (Zöller et al., 2022).

At the Smykiv site, soil veins disturbed the Pryluky and Kaydaky soils and were presumably formed during MIS 5d, MIS 5b, and at the very beginning of MIS 4. The oldest soil veins are the smallest (<1 m); however, in other LPSs of western Ukraine they can reach up to 2 m in depth (Jary, 2009). The lack of ice-wedge pseudomorphs of MIS 5d in western Ukraine testifies to deep seasonal freezing and not to permafrost. Soil veins of MIS 5b are the largest ones in the Smykiv section (up to 1.5 m) and are bent by solifluction. Cryogenic features at this level are rarely distinguished in the sections of western Ukraine, probably due to the truncation of the Upper Horokhiv soil and superimposition of MIS 4 cryogenesis on the older one. However, the presence of solifluction levels and soil veins inside MIS 5 has been proved recently in several LPSs of western Ukraine (Bogucki et al., 2012; Jary and Ciszek, 2013; Łanczont et al., 2014; Bonchkovskyi, 2020a). The cryogenesis during MIS 5b (as during MIS 5d) presumably took place under deep seasonal freezing since both solifluction (Matsuoka, 2001) and soil veins (Romanovskiy, 1993) are not reliable indicators of permafrost. Soil veins of MIS 4 are very narrow and were formed prior to when ice-wedges grew and solifluction took place, as the solifluction horizon overlies them. The lower part of the loesses of MIS 4 (Uday unit) and MIS 2 (Bug unit) are disturbed by solifluction, identifying a more humid climate in the first half of these stadial periods.

Loading structures are observed in the alluvium of MIS 6, which is characteristic of the nearest LPSs, where various forms of periglacial phenomena occur. Occasional faults associated with cryoturbation were probably caused by local permafrost thaw (Van Vliet-Lanoë et al., 2017).

Models of magnetic enhancement and dissolution in LPSs

Magnetic susceptibility as an indicator of paleoclimate change was first used by Heller and Liu (1982, 1984) during magnetic investigations of several loess profiles near Luochuan, China. Further, at numerous sequences located mostly within the Eurasian temperate belt, including Ukraine, it was proved that the variation of high and low values of magnetic susceptibility is closely correlated with paleosol/loess alternation and can be linked directly to the marine oxygen isotope record (Heller et al., 1991; Maher and Thompson, 1992; Forster and Heller, 1994; Maher, 1998; Tsatskin et al., 1998; Jordanova and Petersen, 1999; Panaiotu et al., 2001; Buggle et al., 2009; Marković et al., 2011). Thus, the deposition of these sequences followed the so-called pedogenic ("Chinese") magnetic enhancement model, namely the formation of pedogenic, single-domain, and SP magnetite (and maghemite) grains in paleosols (Hus and Han, 1992; Maher and Thompson 1992).

On the other hand, the magnetic measurements reported from loess sections in Alaska (Begét, 1996; Liu et al., 1999; Muhs et al., 2003) revealed the opposite ("Alaskan" or reducing-pedogenic; Liu and Mao, 2021) pattern: the magnetic susceptibility values are much lower in paleosol samples, and the loesses are characterized by very high values. This was explained by the influence of wind intensity in glacial periods, resulting in the enrichment of coarser grained magnetic minerals in the units of coarse-grained loess (Evans, 2001), and by waterlogging of the soils during interglaciations (Begét et al., 1990; Liu et al., 1999). The gleying process in the redox weathering environment destroys the magnetite (Maher, 1998; Nawrocki et al., 1996; Grimley and Arruda, 2007). This type of paleoclimate record also occurs in inland loesses of North America (Hayward and Lowell, 1993) and some southern Siberian regions (Chlachula et al., 1998; Zhu et al., 2003).

Features of both magnetic enhancement models can be observed at some sites within classic "Chinese" and "Alaskan" model regions. For instance, in the Chinese Loess Plateau (Liu and Mao, 2021), Dnipro Lowland in Ukraine (Hlavatskyi et al., 2023), and Pannonian Plain in Hungary (Sartori et al., 1999; Sümegi et al., 2018), magnetic susceptibility may decrease in paleosols due to gleying processes caused by local geomorphological conditions (location of these sequences in lowlands with a high ground water position). Magnetic susceptibility can also be affected by loess provenance (Grimley et al., 1998). Paleosols of the Great Plains in the central United States have been shown to have either enhanced or reduced magnetic susceptibilities depending on paleodrainage conditions (Grimley et al., 2003; Wang et al., 2009). In many cases, the upper solum of paleosols has increased magnetic susceptibility values while the lower solum can have decreased magnetic susceptibility, compared with the parent loess. Observations of magnetic susceptibility in modern soils has helped to document dissolution processes as an important factor in poorly drained modern soils (de Jong

https://doi.org/10.1017/qua.2024.51 Published online by Cambridge University Press

et al., 2000; Hanesch and Scholger, 2005; Grimley and Arruda, 2007; Blundell et al., 2009) that could be applicable to paleosols. Thus, in addition to climatic conditions, the local and regional factors such as waterlogging, changes in parent material, and soil drainage significantly impact the soil magnetic susceptibility pattern.

Preliminary magnetic susceptibility studies of Polish and western Ukrainian loess sections revealed that their magnetic susceptibility variations are similar to those in the Alaskan sequences (Nawrocki, 1992; Nawrocki et al., 1996, 1999). Hlavatskyi et al. (2016) noticed that the observed enviromagnetic patterns of the Boyanychi and Korshiv sections do not fit the Chinese or Alaskan types of formation of magnetic properties alone: both the loess and paleosol units have higher and lower susceptibility values. Following more comprehensive rock magnetic investigations, Bakhmutov et al. (2017) established that the sections had the pedogenic (Chinese) type of formation of magnetic properties with an admixture of the Alaskan type. Analogous transitional patterns were also reported in the LPSs in Argentina (Bidegain et al., 2009), Pakistan (Akram et al., 1998), and Australia (Ma et al., 2013).

The loess-paleosol deposits at the Smykiv site are characterized by low magnetic susceptibility values ($<20 \times 10^{-8}$ m^3/kg), similar to those at the nearby Korshiv and Boyanychi loess sections ($<24 \times 10^{-8}$ m^3/kg). At the studied loess sequences in northwestern Ukraine, ratios of the magnetic susceptibility of paleosols ($\chi_{lf\ soils}$) divided by that of loess samples ($\chi_{lf\ loess}$) are in the range of 2^{-1} to 3, with a median of from 1.5^{-1} to 1. A few Upper Pleistocene sequences in central Europe, for instance, Biały Kościół in Poland (Moska et al., 2019), Paks in Hungary (Sartori et al., 1999), located to the west of the Volyn Upland, and the Medzhybizh section in the Podillia Upland (200 km SE from Smykiv; Bakhmutov et al., 2018; Hlavatskyi et al., 2021), show similar patterns (Fig. 12).

Moving towards the east and south across the Eurasian loess belt, magnetic susceptibility values increase in loesses, and much more in paleosols. The χ_{lf} values in paleosols are usually two to five times greater than those in loess layers at other sites in Ukraine, the Danube basin, Central Asia, and the Chinese Loess Plateau. In the westernmost part of Ukraine, the pedogenic ("Chinese") model is observed first at the loess sections located within the Middle Dniester basin (Neporotove 7; Hlavatskyi et al., 2022) and in the northernmost part of Ukraine within the Dnipro Upland (e.g., Muzychi; Vigilyanskaya, 2002) (see Fig. 1). In contrast, the magnetic susceptibility values of Alaskan loesses are (on average) three to four times higher than those in paleosols (Liu et al., 1999), and their absolute values are comparable to the highest ones in Eurasia (Fig. 12).

ARM, ARM/IRM$_{1T}$, and χ_{ARM}/χ_{lf} values are relatively higher in paleosol samples (Fig. 7), which contain a higher fraction of SSD particles (in contrast to the loesses). Furthermore, based on the magnetic susceptibility variation pattern, the Smykiv section cannot be classified as having the Chinese type of formation of magnetic properties in the sediments: in many paleosol units, very low magnetic susceptibility values are observed (Fig. 7), indicating the impact of the Alaskan magnetic enhancement model in the formation of the soils. Nevertheless, the loess units in all Ukrainian sections studied, according to magnetic characteristics, have a certain similarity. The mean values of magnetic susceptibility in the loess beds vary within a narrow range of 6 to 15×10^{-8} m^3/kg (Rousseau et al., 2001, 2011; Nawrocki et al., 2002; Bokhorst et al., 2009; Buggle et al., 2009; Bakhmutov et al., 2017, 2018; Hlavatskyi and Bakhmutov, 2020, 2021), with the exception of the Kurortne section on the Black Sea coast

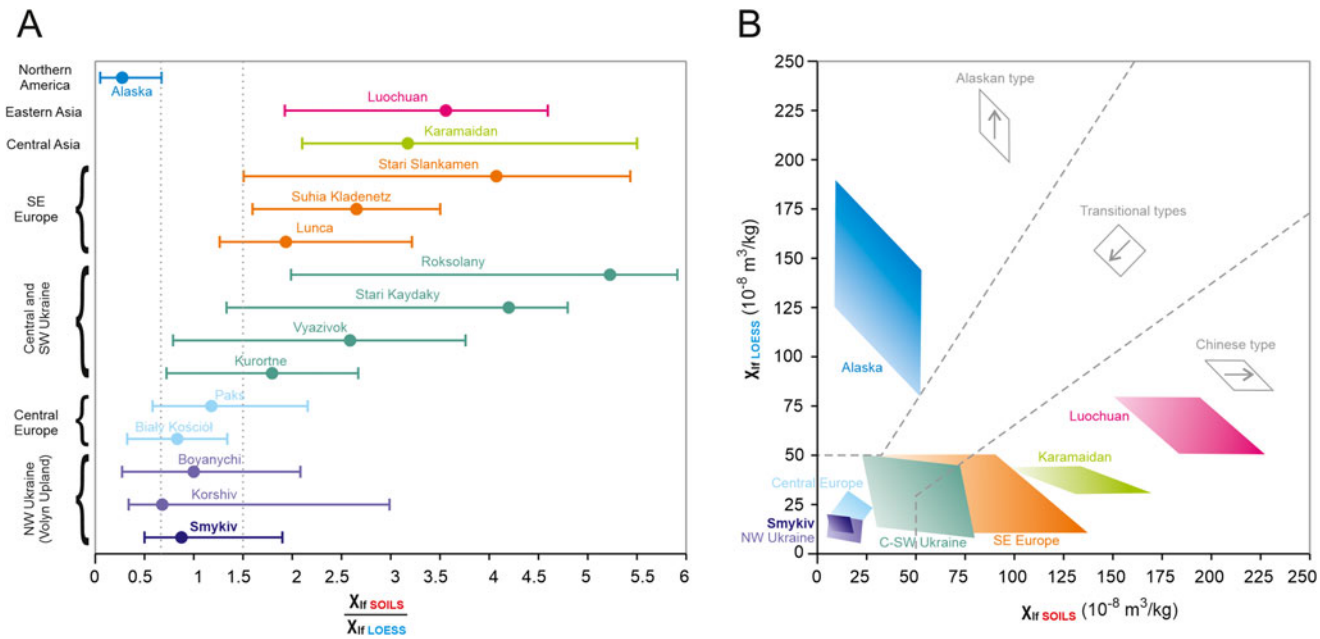

Figure 12. (A) Ratio of magnetic susceptibility in MIS 5 soils divided by that of MIS 2–4 loesses for selected Upper Pleistocene sequences in Eurasia and Alaska; circles = medians; whiskers = ranges of values; and (B) schematic range plots of absolute values of magnetic susceptibility in MIS 5 soil versus MIS 2–4 loess layers. The data were adapted from the following sources: Smykiv (this study), Korshiv and Boyanychi (Hlavatskyi et al., 2016), Kurortne (Tecsa et al., 2020), Vyazivok and Roksolany (Hlavatskyi and Bakhmutov, 2020), Stari Kaydaky, Ukraine (Buggle et al., 2009); Biały Kościół, Poland (Moska et al., 2019); Paks, Hungary (Sartori et al., 1999); Lunca, Romania (Constantin et al., 2015); Suhia Kladenetz, Bulgaria (Jordanova et al., 2022); Stari Slankamen, Serbia (Marković et al., 2011); Karamaidan, Tajikistan (Forster and Heller, 1994); Luochuan, China (Heller et al., 1991); Alaska (Liu et al., 1999). See explanation in the text.

https://doi.org/10.1017/qua.2024.51 Published online by Cambridge University Press

($30–50 \times 10^{-8}$ m^3/kg; Tecsa et al., 2020). This supports the suggestion of a common distal source for the aeolian (loess) material supplied to the entire territory of Ukraine, including the Volyn Upland (Buggle et al., 2008; Bakhmutov et al., 2017).

In addition to contrasting magnetic susceptibility values in paleosol units between the northern and southern Ukrainian sections, differences are observed in magnetic hardness of the rock material. As an illustration, in the Roksolany and Dolynske sections in southern Ukraine, the hematite (and goethite) concentrations are very low, expressed by S values close to 1 (Bakhmutov et al., 2017; Hlavatskyi and Bakhmutov, 2021). The hematite (goethite) concentration in the Smykiv, Boyanychi, Korshiv, and partly Vyazivok sections is significantly higher (Bakhmutov et al., 2017; Hlavatskyi and Bakhmutov, 2020). This is indicated by the lower S values (in particular, in the solifluction horizons) and higher HIRM values, as compared to those at the Roksolany and Dolynske sections. The presence of hematite in the Boyanychi section was established by magnetic mineralogy methods (Nawrocki et al., 1996). In sediments of the Smykiv, Boyanychi, and Korshiv sections, hematite could be formed through the surface oxidation of large magnetite grains.

Therefore, the Upper Pleistocene deposits in northwestern Ukraine were formed in different conditions than those in southern Ukraine. Bakhmutov et al. (2017) suggested that periodic humidification in the territory of the Volyn Upland due to closeness to the ice sheet facilitated the oxidation of the ferrimagnetic grains and the formation of highly coercive minerals. Nevertheless, the majority of the paleosols at Smykiv are not gleyed, though they are sandy. In our view, the supply of hard magnetic material from the nearby alluvial layers is a probable contributory factor. The SP grains of magnetite and maghemite in paleosols could be destroyed by physical and chemical weathering, in particular, blowing winds and erosion which fashioned sedimentary soils, indicated by high $\chi_{fd\%}$ percentages (in most cases) and secondary gleying, observed in a few soil horizons (Table 1) with lower $\chi_{fd\%}$ values. This is well demonstrated by the difference between the IRM acquisition curves of the MIS 5e and Holocene soils: in the MIS 5e soil, oxidized magnetite resulted in the formation of hematite under weathering processes, whereas the classic pedogenic model of the formation of magnetite is observed only in the Holocene soil (Fig. 8D).

Based on the above estimations, we suggest that the Upper Pleistocene LPSs, in general, can be attributed to three types of paleoenvironments based on a few simple criteria presented in Table 4. The northwestern Ukrainian loess sections including the Smykiv section, in our interpretation, belong to the transitional model of the paleoclimate record.

Paleoenvironmental reconstructions

In the loess-paleosol sequence of northwestern Ukraine, seven paleoenvironmental periods, covering the interval since MIS 6 to the final part of MIS 2, have been identified using lithologic, paleopedological, sedimentologic, palynological, and magnetic proxies. In this section, we discuss paleoenvironmental reconstructions for each period in view of the new results obtained from the Smykiv and nearby sites, studied by our team, versus previous data from the central Ukrainian and some European loess sequences. The chronology of the periods is presented for marine isotope stages as in Lisiecki and Raymo (2005) and Wolhfarth (2013).

MIS 6 (Dnipro period; 191–130 ka)

The Dnipro period is associated with the maximum ice-sheet advancement in central Ukraine (Veklych, 1968; Matoshko, 2011). In northwestern Ukraine, the Saalian (Dnieperian) ice sheet reached the northern margins of the Volyn Upland (Godzik et al., 2012) and, in southwestern Poland, the Carpathian foothills (Marks, 2023). In the periglacial areas, high loess sedimentation rates occurred (Rousseau et al., 2020). In the LPSs of northwestern Ukraine, the corresponding loess unit L2 is predominantly 2–3 m thick (Bogucki, 1986; Fedorowicz

Table 4. The proposed criteria for dividing the Upper Pleistocene loess-paleosol sequences based on types of formation of magnetic properties.

Model of magnetic enhancement	$X_{lf\ soils}/\chi_{lf\ loess}$	$X_{lf\ soils}$	$\chi_{lf\ loess}$	Dominant magnetic minerals	Main mechanism	Regions of distribution	References
Alaskan	$<1.5^{-1}$	$<50 \times 10^{-8}$ m^3/kg	$80–190 \times 10^{-8}$ m^3/kg	Magnetite, maghemite	Strong winds, waterlogging	North America, Siberia	Begét et al. (1990); Hayward and Lowell (1993); Liu et al. (1999); Chlachula et al. (1998); Zhu et al. (2003)
Transitional	$1.5^{-1}–1.5$	Usually $<50 \times 10^{-8}$ m^3/kg		Hematite, goethite	Physical and chemical weathering	Northern and central Europe, northwestern Ukraine, Australia, Middle East, Argentina	Nawrocki et al. (1996); Akram et al. (1998); Bidegain et al. (2009); Ma et al. (2013); Bakhmutov et al. (2017); Bradák et al. (2021b); this study
Chinese	>1.5	$50–225 \times 10^{-8}$ m^3/kg	$<80 \times 10^{-8}$ m^3/kg	Magnetite, maghemite	Pedogenic processes	China, Central Asia, southeastern Europe, Ukraine, Africa	Heller and Liu (1982, 1984); Heller et al. (1991); Maher and Thompson (1992); Forster and Heller (1994); Maher (1998); Tsatskin et al. (1998); Jordanova and Petersen (1999); Panaiotu et al. (2001); Buggle et al. (2009); Marković et al. (2011); Hlavatskyi and Bakhmutov (2020, 2021)

https://doi.org/10.1017/qua.2024.51 Published online by Cambridge University Press

et al., 2013; Bogucki and Voloshyn, 2014), reaching up to 5–7 m in some sections (Bogucki and Voloshyn, 2008). At the Novyi Tik site, the geochemistry of L2 differs from other loess units, particularly in its high values of trace elements such as Zr, Ga, Ce, Y and Yb, which are supposed to be the result of another source of aeolian dust at that time (Bonchkovskyi et al., 2023b). For instance, in central Ukraine, sorted fluvioglacial sands are considered to be the main source of dust contributed to the formation of L2 and therein Zr accumulation (Buggle et al., 2008).

At the Novyi Tik and Boremel-2 sites, the reddish laminated sands overlying L2 are considered to be aeolian and originated from the Styr river valley (Bonchkovskyi et al., 2023b). Similar aeolian sands have also been reported in the Korshiv section (Fedorowicz et al., 2013), indicating dynamic aeolian processes at the end of MIS 6. The alternation of coarse-grained sand and silt in the Novyi Tik and Boremel-2 sections may indicate a seasonal variation in wind intensity as documented in the modern periglacial environment (Bateman, 2013). The prevalence of tundra-steppe vegetation (Gerasimenko, 2004) and the existence of permafrost (Dolecki, 2003) presumably conditioned the high wind intensity. At the Smykiv site, the sands overlying the periglacial alluvium can be also defined as aeolian.

MIS 5e (Kaydaky period; 130–111 ka)

The humid and warm climate contributed to the spread of soils with a developed Bt horizon across almost the entire northern European loess belt (Morozova, 1981). The soils are predominantly classified as Luvisols, which are replaced by Retisols in the northern sites of the eastern European Plain (Sycheva et al., 2020; Makeev et al., 2024). In northwestern Ukraine, Retisols were formed on sands, whereas Luvisols were formed on loess.

The most complete LPSs show a similar pattern of soil evolution by the end of the last interglaciation, which in some publications is interpreted as a local phenomenon (Łanczont and Boguckyj, 2007). In the eastern LPSs of Ukraine, there is a cyclicity of pedogenic processes, manifested in two early phases of clay illuviation and two late phases of humus accumulation (Gerasimenko, 2004, 2006; Gerasimenko and Rousseau, 2008). In northwestern and western Ukraine, the same pattern has not yet been traced. However, at the Novyi Tik site, the final phase of the last interglaciation is marked by a humified soil with a steppe palynological assemblage (Bonchkovskyi, 2020a).

Our pollen studies of the Novyi Tik site are in line with previous investigations (Komar et al., 2009, 2015; Łanczont et al., 2022), which reveal an Eemian pollen succession characteristic for central Europe (Mamakowa, 1989). In northwestern Ukraine, the following phases have been distinguished: (1) E1, birch forests; (2) E2, mixed forests; (3) E3, oak–elm–hornbeam forests; (4) E5, spruce–hornbeam forests; (5), mesophytic steppes with elm–birch woodland; (6) E7, pine forests.

MIS 5d (Tyasmyn period; 111–107 ka)

The deterioration of climatic conditions during MIS 5d led to increased erosion and the consequent truncation of the underlying soils, which has been described for the Herning stade in many parts of Europe (Antoine et al., 2016; Sycheva et al., 2020; Adameková et al., 2021). At a higher topographical position, loess-like sandy loams were accumulated and subsequently reworked by pedogenesis or denudated.

As evidenced by cryogenic phenomena (involutions, soil veins, and post-cryogenic textures), cryogenesis presumably occurred under deep seasonal freezing conditions, enhanced by a moisture deficit. The latter is confirmed by the almost absence of solifluction and the appearance of involutions only in relief depressions. Moreover, cryogenesis contributed to the diagenesis of the Eemian soil, for instance in the acquisition of platy peds, cryogenic sorting, and frost heaving.

MIS 5c (Early Pryluky period; 107–88 ka)

The alternation of interstadial and stadial periods contributed to the formation of several soils in the MIS 5c substage. The soil succession is as follows (Bonchkovskyi, 2019, 2020a): forest soils (Podzols, Retisols, Luvisols) of the early optimum phase (pl_{1b1}), strongly humified soil (Phaeozems) of the late optimum phase (pl_{1b2}), and brown soils (Cambisols) or incipient soils (Regosols) of the late phase (pl_{1c}). In places, the soils are separated by thin silt layers, similar to those defined as marker silts at the Dolní Věstonice site in central Europe (Kukla, 1977), which are considered to be the result of strong dust storms (Rousseau et al., 2013).

Palynological data from the nearby Kolodezhi section (Fig. 13) enabled the reconstruction of birch–pine forests in the early optimum phase (pl_{1b1}) and meadow-steppe vegetation in the late optimum phase (pl_{1b2}). Similar data were obtained at the Novyi Tik site, where an admixture of broadleaved trees was registered in the early optimum phase (pl_{1b1}) (Bonchkovskyi, 2020a). In the late phase (pl_{1c}), meadow steppes dominated with patches of pine and birch forests.

The MIS 5c soils in the southern part of the Volyn Upland are characterized by increased sand content and low values of Ti/Zr, Ti/Nb, and Ce/Y ratios (Bonchkovskyi et al., 2023b), which may indicate that the soils could have inherited their texture from parent material (including of aeolian origin) or even that the aeolian sand contributed to pedogenesis. The source of the aeolian sands was presumably the alluvium of the Styr river.

MIS 5b (Middle Pryluky period; 88–85 ka)

The cooling of pl_2 (MIS 5b) is marked by accelerated cryogenesis, probably under deep seasonal freezing. Widespread solifluction indicates a higher humidity compared to the Herning stade. The presence of bent soil veins presumably evidences cracking before solifluction occurs. The MIS 5b unit at the Novyi Tik and Boremel-2 sites is represented by thin loess beds overlain by aeolian sands, associated with soil and sand veins.

MIS 5a (Late Pryluky period; 85–71 ka)

The soils of MIS 5a are represented mainly by dark humified or brown forest soils; however, in the Smykiv section it includes two soils showing a trend towards aridification by the end of MIS 5. The palynological assemblage from the MIS 5a soil (Kolodezhi site) testifies to the spread of meadow-steppe vegetation with patches of lime and pine forests. Numerous krotovinas in the subsoil at the Novyi Tik site (Bonchkovskyi, 2020a) also evidence steppe vegetation. The abrupt decrease in sand content in the uppermost MIS 5a soil testifies to the drastic change in sedimentary environment until the end of MIS 5.

MIS 4 (Uday period; 71–57 ka)

A predominantly thin loess with a higher proportion of clay was formed in the Uday period, probably as a result of the recycling of

https://doi.org/10.1017/qua.2024.51 Published online by Cambridge University Press

older clayey material (Van Loon, 2006), and/or a more remote dust source (Pye, 1995), and/or a decrease in aeolian silt accumulation (Gerasimenko, 2006). A genuine loess was accumulated in the Styr river valley due to its proximity to the dust source—the river valley.

The cold and wet climate of the Uday period contributed to active cryogenesis and permafrost aggradation as evidenced by the ice-wedge pseudomorphs. Ice-wedge bodies presumably melted prior to the MIS 3 interstadial phases (Jary, 2009). At the beginning of the Uday period, solifluction was widespread, contributing to the redeposition of the Pryluky soils.

Palynological data from the Novyi Tik site revealed typical tundra vegetation featuring dwarf birch (*Betula* sect. Nanae) and shrub alder (*Alnus alnobetula* subsp. *fruticosa*) (Bonchkovskyi, 2020a). Bezusko et al. (2011) suggested that open coniferous and birch forests could have existed in the river valleys.

MIS 3 (Vytachiv period; 57–27 ka)

The Vytachiv soil at the Smykiv site is a polygenetic Gleyic Cambisol formed rather under boreal vegetation. Thin overlying tundra gley indicates periglacial pedogenesis at the very end of MIS 3. At the Kolodezhi site (Fig. 13), three Vytachiv soils represent a typical soil succession described in central Ukraine (Gerasimenko, 2006) and show at least three interstadial phases. In the second half of the first interstadial phase (vt_{1b1}), Gleysols were formed in the boreal forest-steppe, where meadow steppes alternated with birch–pine forests. However, in the early phase, this soil was presumably formed under periglacial or subperiglacial vegetation (Gurtovaya, 1985). In the second interstadial phase (vt_{1b2}), Cambisols were formed under boreal mixed forests dominated by birch and pine, with broadleaved trees (oak, hornbeam, hazel) as an admixture. In the youngest interstadial phase (vt_{3b}), carbonate brown soils (Regosols) were formed under boreal open pine forests and meadow steppes with a slight admixture of xerophytes.

MIS 2 (Bug–Prychornomorya period; 27–10 ka)

In northwestern Ukraine, the thickest loess was formed during the Late Pleniglacial (MIS 2) (Bogucki, 1986; Jary and Ciszek, 2013) with two distinct tundra gleys designated as the Rivne and Krasyliv units (Bogucki, 1986), representing short, relatively warm periods (Łanczont and Madeyska, 2015). The micromorphology of the loess from the Smykiv site indicates relatively high biological activity during loess accumulation, which suggests the spread of relatively rich herbaceous vegetation at this time. According to palynological data, periglacial steppe and tundra-steppe with cryophytes and xerophytes occurred (Bezusko et al., 2010).

Increased aridity towards the end of the Late Pleniglacial led to the disappearance of solifluction, which was widespread at the beginning of MIS 2. In return, the largest ice-wedge casts grew under continuous permafrost, presumably during the Heinrich event H1 (Fedorowicz et al., 2018) or were associated with the Krasyliv period (Bogucki, 1986).

Relatively warm phases (Rivne and Krasyliv periods) are represented by tundra gleys. On drained surfaces, the lower Dofinivka (Rivne) tundra gley turn into incipient brown soils as evidenced by the Regosol at the Smykiv site. At the nearby Kolodezhi site, a pollen assemblage from the Regosol enables the reconstruction of boreal meadow steppes (Fig. 13). Similar steppe vegetation with patches of open pine–birch forests with a slight admixture of lime was reconstructed at the Novyi Tik site (Bonchkovskyi, 2020a). The Krasyliv tundra gley was presumably formed under subperiglacial or periglacial vegetation, indicating weak warming.

The general scheme of paleoenvironmental reconstruction is given in Figure 14. This displays considerable paleoenvironmental changes, demonstrating a general trend towards cooling and aridification from MIS 5 to MIS 2. The last interglacial (MIS 5e) was most similar to the modern one, but was characterized by higher humidity. The warmest interstadials of MIS 5 and MIS 3 were characterized by southern-boreal landscapes, whereas boreal

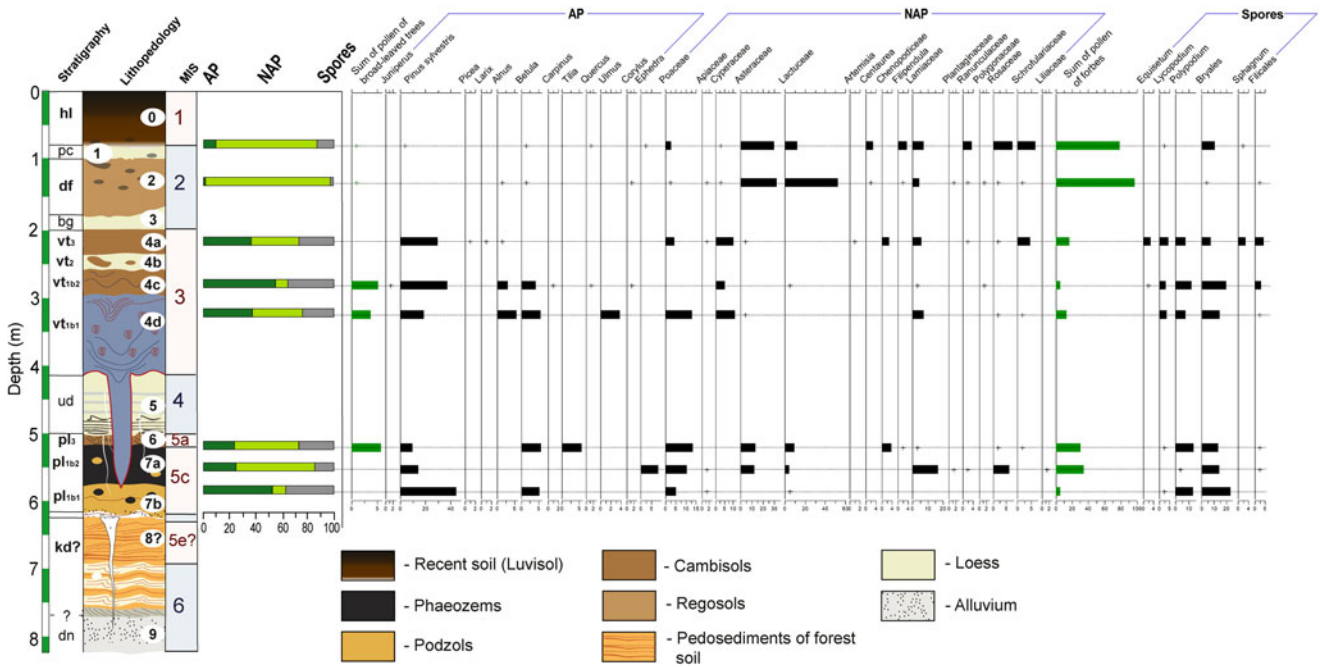

Figure 13. Pollen diagram for the Kolodezhi site (this study). AP, arboreal pollen; NAP, non-arboreal pollen.

https://doi.org/10.1017/qua.2024.51 Published online by Cambridge University Press

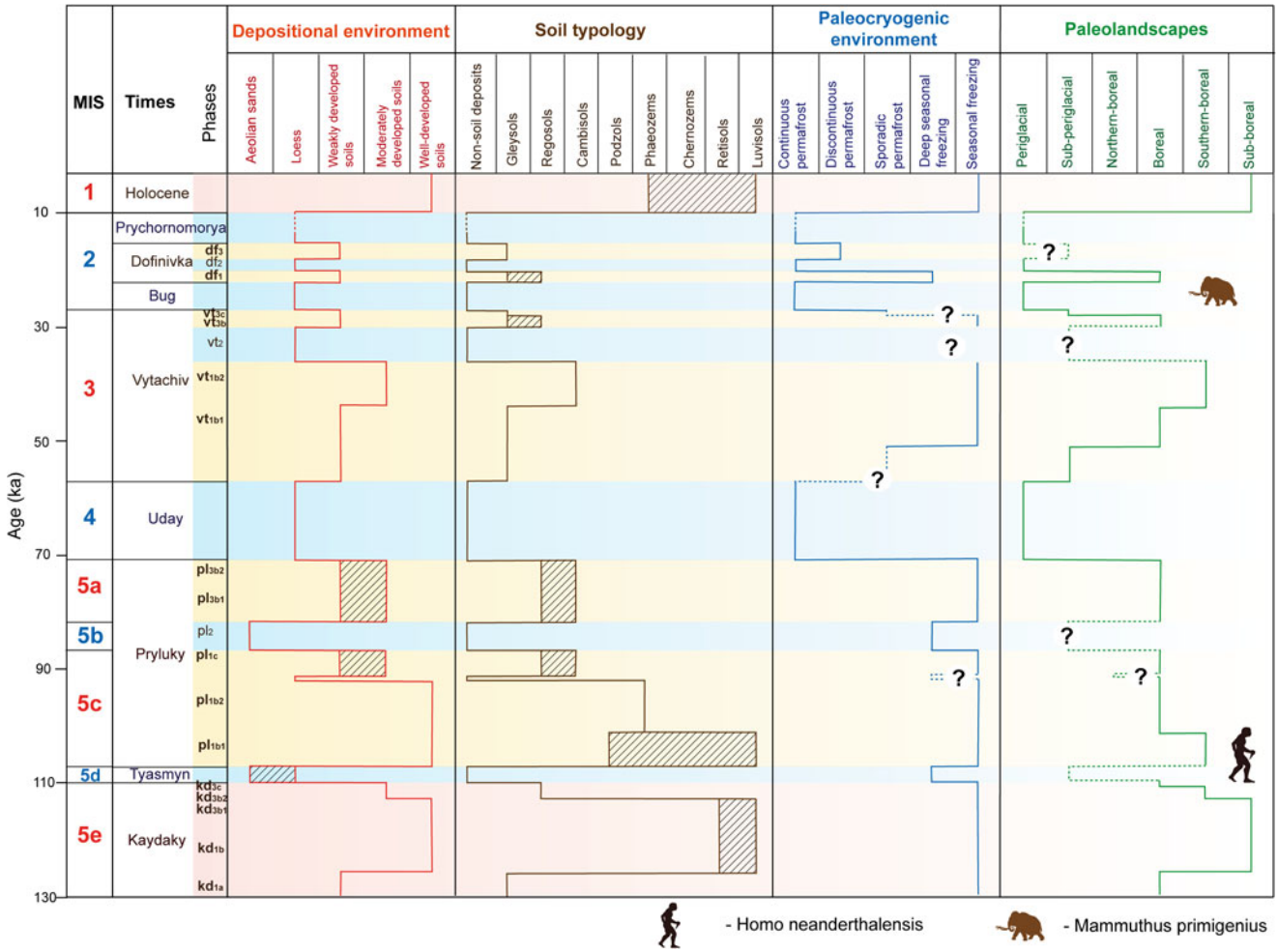

Figure 14. Regional paleoenvironmental reconstructions for northwestern Ukraine based on the data from the Smykiv (this study), Novyi Tik (Bonchkovskyi, 2020a), and Kolodezhi (this study) loess-paleosol sequences. *Homo neanderthalensis* and *Mammuthus primigenius* are given after Bonchkovskyi (2020a).

landscapes occurred even during the interstadials of MIS 2 (Rivne).

Conclusions

The loess-paleosol sequence of northwestern Ukraine shows developed interglacial and interstadial paleosols and relatively thin loess units. The loess units bear signs of redoximorphic features, solifluction, involution, and developed ice-wedge pseudomorphs, indicating the wet first and dry second half of the stadials. The pedocomplex of MIS 5 comprises four soils (from Retisol to Phaeozem and Calcaric Regosol), demonstrating a trend towards cooling and aridification. Owing to the erosional phases occurring in the stadial periods, the soils are partly truncated. The sandy texture of the MIS 5 soils indicates the contribution of aeolian sand sedimentation to pedogenesis and/or high rates of aeolian sand sedimentation during the cold periods of MIS 5. A shift in sedimentation can be traced in MIS 5a as a response to river valley reshaping. The MIS 3 soil is represented by Gleyic Cambisol, indicating the predominance of boreal landscapes during interstadial periods, whereas the main soil of MIS 2 is less developed (Calcaric Gleyic Regosol), formed under boreal landscapes during a short warm period at 21–23 ka.

Magnetic data from the Smykiv and nearby loess-paleosol sections support the hypothesis of the transitional model (containing aspects of both the "Chinese" and "Alaskan" models) of magnetic enhancement in northwestern Ukraine. However, the relative impacts of different mechanisms of physical and chemical weathering on the destruction of magnetite (and maghemite) grains in paleosols, as well as the origin of magnetic material in loess and pedosediments, has been reconsidered in terms of proximate sources of supply.

In comparison with other European LPSs, the Upper Pleistocene sequence in northwestern Ukraine is more similar to those of the central European loess subdomain (pronounced redoximorphic features in loess units, well-developed periglacial phenomena, and low magnetic susceptibility values in paleosols) rather than the eastern European loess subdomain. We conclude that the boundary between the two subdomains should be located 250 km further east than previously suggested (Lehmkuhl et al., 2021). The high variability of coeval soils and changes in pedogenesis during the Late Pleistocene support that pedogenesis and paleolandscapes are more sensitive to climate change in transitional zones and ecotones. This record also suggests a dissolution mechanism for the transitional model of magnetic enhancement.

Additional studies, including radiocarbon and luminescence dating, as well as malacological and geochemical studies, are

https://doi.org/10.1017/qua.2024.51 Published online by Cambridge University Press

needed to obtain a robust chronostratigraphy of the studied sequence.

Acknowledgments. The study was partly supported by the National Research Foundation of Ukraine, grant number 2020.02/0406 (50%), Ministry of Education and Science of Ukraine, project No. 22BF050-01 (40%; O. Bonchkovskyi), and by a budget allocation from the National Academy of Sciences of Ukraine for research work 0124U000085 (10%; D. Hlavatskyi). The authors thank T. Skarboviychuk, L. Dyachuk, and S. Cherkes for their help with the rock magnetic measurements. We are thankful to Prof. S. Marković and two anonymous reviewers for their helpful and inspiring comments.

References

Adameková, K., Lisá, L., Neruda, P., Petřík, J., Doláková, N., Novák, J., Volánek, J., 2021. Pedosedimentary record of MIS 5 as an interplay of climatic trends and local conditions: multi-proxy evidence from the Palaeolithic site of Moravský Krumlov IV (Moravia, Czech Republic). *Catena* **200**, 105174. https://doi.org/10.1016/j.catena.2021.105174

Akram, H., Yoshida, M., Ahmad, M.N., 1998. Rock magnetic properties of the late Pleistocene Loess-Paleosol deposits in Haro River area, Attock basin, Pakistan: is magnetic susceptibility a proxy measure of paleoclimate? *Earth, Planets and Space* **50**, 129–139.

Antoine, P., Coutard, S., Guerin, G., Deschodt, L., Goval, E., Locht, J.-L., Paris, C., 2016. Upper Pleistocene loess-palaeosol records from Northern France in the European context: environmental background and dating of the Middle Palaeolithic. *Quaternary International* **411**, 4–24.

Antoine, P., Rousseau, D.-D., Degeai, J.-P., Moine, O., Lagroix, F., Kreutzer, S., Fuchs, M., *et al.*, 2013. High-resolution record of the environmental response to climatic variations during the Last Interglacial–Glacial cycle in Central Europe: the loess-palaeosol sequence of Dolní Věstonice (Czech Republic). *Quaternary Science Reviews* **67**, 17–38.

Aquino, A., Scardia, G., Prud'homme, C., Dave, A.K., Lezzerini, M., Johansson, A.E., Marquer, L., Safaraliev, N., Lauer, T., Fitzsimmons, K.E., 2024. Variability in geochemical weathering indices in loess over the last full glacial cycle at Karamaidan, central Asia (Tajikistan). *Frontiers in Earth Science* **12**, 1347910. https://doi.org/10.3389/feart.2024.1347910

Bakhmutov, V., Hlavatskyi, D., Poliachenko, I., 2023. Magnetostratigraphy of the Pleistocene loess-palaeosol sequences in Ukraine and Moldova: a historical overview and recent developments. *Geological Quarterly* **67**, 35. https://doi.org/10.7306/gq.1705

Bakhmutov, V., Hlavatskyi, D., Stepanchuk, V., Poliachenko, I., 2018. Rock magnetism and magnetostratigraphy of loess-palaesol sections – Lower Paleolithic sites of Podolian Upland (Medzhybizh, Holovchintsi). In: *12th International Scientific Conference "Monitoring of Geological Processes and Ecological Condition of the Environment."* European Association of Geoscientists & Engineers, pp. 1–5.

Bakhmutov, V.G., Kazanskii, A.Y., Matasova, G.G., Glavatskii, D.V., 2017. Rock magnetism and magnetostratigraphy of the loess-sol series of Ukraine (Roksolany, Boyanychi, and Korshev sections). *Izvestiya, Physics of the Solid Earth* **53**, 864–884.

Bateman, M.D., 2013. Aeolian processes in periglacial environments. In: Shroder, J.F. (Ed.), *Treatise on Geomorphology*. Academic Press, San Diego, pp. 416–429.

Becze-Deàk, J., Langohr, R., Verrecchia, E.P., 1997. Small scale secondary $CaCO_3$ accumulations in selected sections of the European loess belt. Morphological forms and potential for paleoenvironmental reconstruction. *Geoderma* **76**, 221–252.

Begét, J.E., 1996. Tephrochronology and paleoclimatology of the Last Interglacial-Glacial cycle recorded in Alaskan loess deposits. *Quaternary International* **34–36**, 121–126.

Begét, J.E., Stone, D.B., Hawkins, D.B., 1990. Palaeoclimatic forcing of magnetic susceptibility variations in Alaskan loess during the late Quaternary. *Geology* **18**, 40–43.

Bertran, P., Stadelmaier, K.H., Ludwig, P., 2022. Last Glacial Maximum active layer thickness in Western Europe, and the issue of 'tundra gleys' in loess sequences. *Journal of Quaternary Science* **37**, 1222–1228.

Bezusko, L.G., Mosyakin, S.L., Bezusko, A.G., 2011. *Patterns and Trends of Development of the Plant Cover of Ukraine in the Late Pleistocene and Holocene*. [In Ukrainian.] Alterpress, Kyiv.

Bezusko, L.G., Mosyakin, S.L., Bezusko, A.G., Boguckyj, A., 2010. Palynological characteristics of the Upper Pleistocene deposits of the Podolian Highland (Ukraine). [In Ukrainian.] *Scientific Notes of NaUKMA. Biology and Ecology* **106**, 23–28.

Bidegain, J.C., Rico, Y., Bartel, A., Chaparro, M.A.E., Jurado, S., 2009. Magnetic parameters reflecting pedogenesis in Pleistocene loess deposits of Argentina. *Quaternary International* **209**, 175–186.

Blundell, A., Dearing, J.A., Boyle, J.F., Hannam, J.A., 2009. Controlling factors for the spatial variability of soil magnetic susceptibility across England and Wales. *Earth-Science Reviews* **95**, 158–188.

Bogucki, A., 1986. Quaternary cover sediments in Volyn-Podillia. In: Makarenko, D.E. (Ed.), *Quaternary Deposits of Ukraine*. [In Russian.] Naukova Dumka, Kyiv, pp. 121–132.

Bogucki, A., Łanczont, M., Tomeniuk, O., Sytnyk, O., 2012. Colluvial-solifluctional processes and problems of redeposition and dating of Paleolithic cultural horizons. [In Ukrainian.] *Materials and Studies on Archaeology of Sub-Carpathian and Volhynian Area* **16**, 55–64.

Bogucki, A., Velichko, A., Nechaev, V., 1975. The paleocryogenic processes in the Western Ukraine during Middle and Late Pleistocene. In: *The Problems of Palaeogeography of Loess and Periglacial Areas*. [In Russian.] Nauka, Moscow, pp. 80–89.

Bogucki, A., Voloshyn, P., 2008. Engineering-geological characteristic of the rocks of the loess-soil series from the key section Rivne (Volhynian Upland). [In Ukrainian.] *Visnyk of Lviv University. Series Geography* **35**, 7–15.

Bogucki, A., Voloshyn, P., 2014. Engineering-geological characteristic of the rocks of the loess-soil series from the key section Boyanychi (Volhynian Upland). [In Ukrainian.] *Visnyk of Lviv University. Series Geography* **47**, 18–29.

Bogucki, A., Voloshyn, P., Tomeniuk, O., 2014. The collapsibility of Pleistocene loess-paleosols and cryogenic levels. [In Polish.] *Przeglad Geoloczny* **62**, 553–559.

Boguckyj, A.B., Łanczont, M., Łącka, B., Madeyska, T., Sytnyk, O., 2009. Age and the palaeoenvironment of the West Ukrainian palaeolithic: the case of Velykyi Glybochok multi-cultural site. *Journal of Archaeological Science* **36**, 1376–1389.

Bogutskiy, A., Łanczont, M., Racinowski, R., 2000. Conditions and course of sedimentation of the Middle and Upper Pleistocene loesses in the Halic profile (NW Ukraine). *Studia Quaternaria* **16**, 3–17.

Bokhorst, M.P., Beets, C.J., Marković, S.B., Gerasimenko, N.P., Matviishina, Z.N., Frechen, M., 2009. Pedo-chemical climate proxies in Late Pleistocene Serbian–Ukrainian loess sequences. *Quaternary International* **198**, 113–123.

Bonchkovskyi, O.S., 2019. Changes in pedogenic processes during Pryluky times (Late Pleistocene) in the central part of the Volyn Upland. *Journal of Geology, Geography and Geoecology* **28**, 230–240.

Bonchkovskyi, O., 2020a. The loess-palaeosol sequence of Novyi Tik: a new Middle and Upper Pleistocene record for Volyn' Upland (North-West Ukraine). *Quaternaire* **31**, 281–308.

Bonchkovskyi, O.S., 2020b. Smykiv – the new key section of the Upper Pleistocene of the Volyn Upland. [In Ukrainian.] *V. N. Karazin Kharkiv National University Bulletin* **53**, 25–44.

Bonchkovskyi, O., Hlavatskyi, D., Kuraieva, I., Kravchuk, I., Bonchkovskyi, A., 2023a. Lithology, geochemistry and magnetic susceptibility of the best developed late Pleistocene loess-palaeosol sequence in north-western Ukraine, Novyi Tik. In: *International Conference of Young Professionals «GeoTerrace-2023»*. European Association of Geoscientists & Engineers, pp. 1–5. https://doi.org/10.3997/2214-4609.2023510099

Bonchkovskyi, O.S., Kuraeva, I.V., Bonchkovskyi, A.S., 2023b. Grain-size and geochemical investigations on the Novyi Tik site (NW Ukraine) and their significance for understanding the local sedimentary environment in the Pleistocene. *Journal of Geology, Geography and Geoecology* **32**, 679–694.

Bradák, B., Csonka, D., Novothny, Á., Szeberényi, J., Medveďová, A., Rostinsky, P., Fehér, K., *et al.*, 2021a. Late Pleistocene paleosol formation in a dynamic aggradational microenvironment – a case study from the Malá

nad Hronom loess succession (Slovakia). *Catena* **199**, 105087. https://doi.org/10.1016/j.catena.2020.105087.

Bradák, B., Seto, Y., Nawrocki, J., 2019. Significant pedogenic and palaeoenvironmental changes during the early Middle Pleistocene in Central Europe. *Palaeogeography, Palaeoclimatology, Palaeoecology* **534**, 109335. https://doi.org/10.1016/j.palaeo.2019.109335.

Bradák, B., Seto, Y., Stevens, T., Újvári, G., Fehér, K., Költringer, C., 2021b. Magnetic susceptibility in the European Loess Belt: new and existing models of magnetic enhancement in loess. *Palaeogeography, Palaeoclimatology, Palaeoecology* **569**, 110329. https://doi.org/10.1016/j.palaeo.2021.110329.

Bronger, A., 2003. Correlation of loess–paleosol sequences in East and Central Asia with SE Central Europe: towards a continental Quaternary pedostratigraphy and paleoclimatic history. *Quaternary International* **106–107**, 11–31.

Buggle, B., Glaser, B., Zöller, L., Hambach, U., Marković, S., Glaser, I., Gerasimenko, N., 2008. Geochemical characterization and origin of Southeastern and Eastern European loesses (Serbia, Romania, Ukraine). *Quaternary Science Reviews* **27**, 1058–1075.

Buggle, B., Hambach, U., Glaser, B., Gerasimenko, N., Marković, S., Glaser, I., Zöller, L., 2009. Stratigraphy, and spatial and temporal paleoclimatic trends in Southeastern/Eastern European loess–paleosol sequences. *Quaternary International* **196**, 86–106.

Chlachula, J., Evans, M.E., Rutter, N.W., 1998. A magnetic investigation of a Late Quaternary loess/palaeosol record in Siberia. *Geophysical Journal International* **132**, 128–132.

Constantin, D., Cameniță, A., Panaiotu, C., Necula, C., Codrea, V., Timar-Gabor, A., 2015. Fine and coarse-quartz SAR-OSL dating of Last Glacial loess in Southern Romania. *Quaternary International* **357**, 33–43.

Dearing, J.A., Dann, R.J.L., Hay, K., Lees, J.A., Loveland, P.J., Maher, B.A., O'Grady, K., 1996. Frequency-dependent susceptibility measurements of environmental materials. *Geophysical Journal International* **124**, 228–240.

de Jong, E., Pennock, D.J., Nestor, P.A., 2000. Magnetic susceptibility of soils in different slope positions in Saskatchewan, Canada. *Catena* **40**, 291–305.

Dolecki, L., 2003. Periglacial structures in loesses of three last glacial cycles (Odranian, Wartanian, Vistulian) in Poland, western Ukraine and southwestern Russian. [In Polish.] *Annales Universitatis Mariae Curie-Sklodowska* **8**, 65–92.

Dzierżek, J., Lindner, L., Chlebowski, R., Szymanek, M., Bogucki, A., Tomeniuk, O., 2022. Depositional conditions of the Upper Younger Loess during the Last Glacial Maximum in central and eastern Europe. *Acta Geologica Polonica* **72**, 369–389.

Dzierżek, J., Lindner, L., Nawrocki, J., 2020. The loess section in Wąchock as the key site of Vistulian loesses and palaeosols in the Holy Cross Mountains (Poland). *Geological Quarterly* **64**, 252–262.

Evans, M.E., 2001. Magnetoclimatology of aeolian sediments. *Geophysical Journal International* **144**, 495–497.

Evans, M.E., Heller, F., 2001. Magnetism of loess/palaeosol sequences: recent developments. *Earth-Science Reviews* **54**, 129–144.

Evans, M.E., Heller, F., 2003. *Environmental Magnetism: Principles and Applications of Enviromagnetics*. Academic Press, San Diego.

FAO, 2006. *Guidelines for Soil Description*. 4th ed. Food and Agriculture Organization of the United Nations, Rome.

Fedoroff, N., Goldberg, P., 1982. Comparative micromorphology of two late Pleistocene paleosols (in the Paris Basin). *Catena* **9**, 227–251.

Fedorowicz, S., Łanczont, M., Bogucki, A., Kusiak, J., Mroczek, P., Adamiec, G., Bluszcz, A., Moska, P., Tracz, M., 2013. Loess-paleosol sequence at Korshiv (Ukraine): chronology based on complementary and parallel dating (TL, OSL), and litho-pedosedimentary analyses. *Quaternary International* **296**, 117–130.

Fedorowicz, S., Łanczont, M., Mroczek, P., Bogucki, A., Standzikowski, K., Moska, P., Kusiak, J., Bluszcz, A., 2018. Luminescence dating of the Volochysk section – a key Podolian loess site (Ukraine). *Geological Quarterly* **62**, 729–744.

Folk, R.L., Ward, W.C., 1957. Brazos River bar [Texas]; a study in the significance of grain size parameters. *Journal of Sedimentary Research* **27**, 3–26.

Forster, Th., Evans, M.E., Heller, F., 1994. The frequency dependence of low field susceptibility in loess sediments. *Geophysical Journal International* **118**, 636–642.

Forster, Th., Heller, F., 1994. Loess deposits from the Tajik depression (Central Asia): magnetic properties and paleoclimate. *Earth and Planetary Science Letters* **128**, 501–512.

Frechen, M., Van Vliet-Lanoë, B., Van den Haute, P., 2001. The Upper Pleistocene loess record at Harmignies/Belgium — high resolution terrestrial archive of climate forcing. *Palaeogeography, Palaeoclimatology, Palaeoecology* **173**, 175–195.

Gerasimenko, N.P., 1997. Natural environment of human habitation in the south-east of Ukraine in the Late Glacial and Holocene (on the materials of paleogeographical study of archaeological monuments). [In Russian.] *Archaeological Almanac* **6**, 3–64.

Gerasimenko, N.P., 2004. The Development of Zonal Landscapes of the Quaternary Period in the Territory of Ukraine. [In Ukrainian.] Doctoral thesis, Taras Shevchenko National University of Kyiv, Kyiv.

Gerasimenko, N., 2006. Upper Pleistocene loess–palaeosol and vegetational successions in the Middle Dnieper Area, Ukraine. *Quaternary International* **149**, 55–66.

Gerasimenko, N.P., 2010a. On the correlation of palaeogeographic stages of the Pleistocene of Ukraine with global benchmarks and chronostratigraphy of Western and Eastern Europe. In: Matviishyna, Z.M., Gerasimenko, N.P., Perederyi, V.I., Bragin, A.M., Ivchenko, A.S., Karmazinenko, S.P., Nagirnyi, V.M., Parkhomenko, O.G. (Eds.), *Spatio-Temporal Correlation of Quaternary Palaeogeographic Conditions on the Territory of Ukraine*. [In Ukrainian.] Naukova Dumka, Kyiv, pp. 94–104.

Gerasimenko, N.P., 2010b. Correlation of short-term palaeoenvironmental changes in the Pleistocene according to palaeolandscape data. In: Matviishyna, Z.M., Gerasimenko, N.P., Perederyi, V.I., Bragin, A.M., Ivchenko, A.S., Karmazinenko, S.P., Nagirnyi, V.M., Parkhomenko, O.G. (Eds.), *Spatio-Temporal Correlation of Quaternary Palaeogeographic Conditions on the Territory of Ukraine*. [In Ukrainian.] Naukova Dumka, Kyiv, pp. 104–129.

Gerasimenko, N.P., 2011. Climatic and environmental oscillations in southeastern Ukraine from 30 to 10 ka, inferred from pollen and lithopedology. In: Buynevich, I.V., Yanko-Hombach, V., Gilbert, A.S., Martin, R.E. (Eds.), *Geology and Geoarchaeology of the Black Sea Region: Beyond the Flood Hypothesis*. Special Paper 473. Geological Society of America, Boulder, CO, USA, pp. 117–132.

Gerasimenko, N., Hlavatskyi, D., Bakhmutov, V., Wimbledon, W.A.P., Poliachenko, I., Bonchkovskyi, O., 2022. Enviromagnetic study of the reference Ukrainian loess-palaeosol sequence at Stari Kaydaky. In: *16th International Conference "Monitoring of Geological Processes and Ecological Condition of the Environment"*. European Association of Geoscientists & Engineers, pp. 1–5. https://doi.org/10.3997/2214-4609.2022580069

Gerasimenko, N., Rousseau, D.-D., 2008. Stratigraphy and paleoenvironments of the last Pleniglacial in the Kyiv Loess Region (Ukraine). *Quaternaire* **19**, 293–307.

Gerenchuk, K.I. (Ed.), 1976. *Nature of Rivne Region*. [In Ukrainian.] Vyshcha shkola, Lviv.

Ghafarpour, A., Khormali, F., Tazikeh, H., Kehl, M., Rolf, C., Frechen, M., Zeeden, C., 2023. Geophysical sediment properties of a late Pleistocene loess–paleosol sequence, Chenarli, northeastern Iran. *Quaternary Research* **114**, 114–129.

Gocke, M., Hambach, U., Eckmeier, E., Schwark, L., Zöller, L., Fuchs, M., Löscher, M., Wiesenberg, G.L.B., 2014. Introducing an improved multiproxy approach for paleoenvironmental reconstruction of loess–paleosol archives applied on the Late Pleistocene Nussloch sequence (SW Germany). *Palaeogeography, Palaeoclimatology, Palaeoecology* **410**, 300–315.

Gozhik, P., Komar, M., Łanczont, M., Fedorowicz, S., Bogucki, A., Mroczek, P., Prylypko, S., Kusiak, J., 2014. Paleoenvironmental history of the Middle Dnieper Area from the Dnieper to Weichselian Glaciation: a case study of the Maksymivka loess profile. *Quaternary International* **334–335**, 94–111.

Gozhik, P., Lindner, L., Marks, L., 2012. Late Early and early Middle Pleistocene limits of Scandinavian glaciations in Poland and Ukraine. *Quaternary International* **271**, 31–37.

Gozhik, P.F., Shelkoplyas, V.N., Komar, M.S., Matviishyna, Z.M., Peredereiy, V.I., 2000. *Guide of the X Polish-Ukrainian Seminar*

https://doi.org/10.1017/qua.2024.51 Published online by Cambridge University Press

"Correlation of Loesses and Ice Deposits." [In Ukrainian.] Institute of Geological Sciences of the National Academy of Sciences of Ukraine, Kyiv.

Grimley, D.A., Arruda, N.K., 2007. Observations of magnetite dissolution in poorly drained soils. *Soil Science* **172**, 968–982.

Grimley, D.A., Follmer, L.R., Hughes, R.E., Solheid, P.A., 2003. Modern, Sangamon and Yarmouth soil development in loess of unglaciated southwestern Illinois. *Quaternary Science Reviews* **22**, 225–244.

Grimley, D.A., Follmer, L.R., McKay, E.D., 1998. Magnetic susceptibility and mineral zonations controlled by provenance in loess along the Illinois and Central Mississippi River Valleys. *Quaternary Research* **49**, 24–36.

Guiter, F., Andrieu-Ponel, V., de Beaulieu, J.-L., Cheddadi, R., Calvez, M., Ponel, P., Reille, M., Keller, T., Goeury, C., 2003. The last climatic cycles in Western Europe: a comparison between long continuous lacustrine sequences from France and other terrestrial records. *Quaternary International* **111**, 59–74.

Guo, J., Shi, J., Chen, H., Song, C., Dong, Q., Wang, W., 2023. Loess strata distribution characteristics and paleoclimate spatial pattern during the Last Interglacial in the Luohe River Basin. *Geosciences* **13**, 158. https://doi.org/10.3390/geosciences13060158.

Gurtovaya, E.E., 1985. Conditions of formation of the Dubno horizon on the northern margin of the Podolia Upland. In: Grichuk, V.P., Zaklinskaya, E.D. (Eds.), *Quaternary Palynology*. [In Russian.] Nauka, Moscow, pp. 147–158.

Haesaerts, P., Borziak, I., Chirica, V., Damblon, F., Koulakovska, L., Van Der Plicht, J., 2003. The east Carpathian loess record: a reference for the middle and late pleniglacial stratigraphy in central Europe. *Quaternaire* **14**, 163–188.

Haesaerts, P., Damblon, F., Gerasimenko, N., Spagna, P., Pirson, S., 2016. The Late Pleistocene loess-palaeosol sequence of Middle Belgium. *Quaternary International* **411**, 25–43.

Hanesch, M., Scholger, R., 2005. The influence of soil type on the magnetic susceptibility measured throughout soil profiles. *Geophysical Journal International* **161**, 50–56.

Hayward, R.K., Lowell, T.V., 1993. Variations in loess accumulation rates in the mid-continent, United States, as reflected by magnetic susceptibility. *Geology* **21**, 821–824.

Heller, F., Liu, T.S., 1982. Magnetostratigraphical dating of loess deposits in China. *Nature* **300**, 431–433.

Heller, F., Liu, T.S., 1984. Magnetism of Chinese loess deposits. *Geophysical Journal International* **77**, 125–141.

Heller, F., Liu, X., Liu, T., Xu, T., 1991. Magnetic susceptibility of loess in China. *Earth and Planetary Science Letters* **103**, 301–310.

Hlavatskyi, D.V., Bakhmutov, V.G., 2020. Magnetostratigraphy and magnetic susceptibility of the best developed Pleistocene loess-palaeosol sequences of Ukraine: implications for correlation and proposed chronostratigraphic models. *Geological Quarterly* **64**, 723–753.

Hlavatskyi, D., Bakhmutov, V., 2021. Early–Middle Pleistocene magnetostratigraphic and rock magnetic records of the Dolynske Section (Lower Danube, Ukraine) and their application to the correlation of loess–palaeosol sequences in Eastern and South-Eastern Europe. *Quaternary* **4**, 43. https://doi.org/10.3390/quat4040043.

Hlavatskyi, D., Bakhmutov, V., Bogucki, A., Voloshyn, P., 2016. Petromagnetism and paleomagnetism of subaerial deposits of Boyanychi and Korshiv sections (Volhynian Upland). [In Ukrainian.] *Visnyk of Taras Shevchenko National University of Kyiv: Geology* **72**, 43–51.

Hlavatskyi, D., Stepanchuk, V., Kuzina, D., Poliachenko, I., Shpyra, V., Skarboviychuk, T., Yakukhno, V., Bakhmutov, V., 2021. Rock magnetic and palaeomagnetic studies of loess-palaeosol sections – Lower Palaeolithic sites within the Southern Bug Valley (Medzhybizh, Holovchyntsi). *Geofizicheskiy Zhurnal* **43**, 3–37.

Hlavatskyi, D., Gerasimenko, N., Bakhmutov, V., Poliachenko, I., 2022. Rock magnetic record from the Late Middle–Upper Pleistocene deposits of the Neporotove 7 loess-soil section (western Ukraine). In: *AGU Fall Meeting 2022, Abstracts*. American Geophysical Union.

Hlavatskyi, D., Gerasimenko, N., Bakhmutov, V., Poliachenko, I., Cherkes, S., 2023. Extremely low magnetic susceptibility in the Lubny (S5, MIS 13) pedocomplex at the type locality Vyazivok (central Ukrainian loess belt). In: *International Conference of Young Professionals «GeoTerrace-2023»*. European Association of Geoscientists & Engineers, pp. 1–5. https://doi.org/10.3997/2214-4609.2023510080

Hošek, J., Hambach, U., Lisá, L., Grygar, T.M., Horáček, I., Meszner, S., Knésl, I., 2015. An integrated rock-magnetic and geochemical approach to loess/paleosol sequences from Bohemia and Moravia (Czech Republic): implications for the Upper Pleistocene paleoenvironment in central Europe. *Palaeogeography, Palaeoclimatology, Palaeoecology* **418**, 344–358.

Hošek, J., Lisá, L., Hambach, U., Petr, L., Vejrostová, L., Bajer, A., Grygar, T.M., Moska, P., Gottvald, Z., Horsák, M., 2017. Middle Pleniglacial pedogenesis on the northwestern edge of the Carpathian basin: a multidisciplinary investigation of the Bíňa pedo-sedimentary section, SW Slovakia. *Palaeogeography, Palaeoclimatology, Palaeoecology* **487**, 321–339.

Hus, J.J., Han, J., 1992. The contribution of loess magnetism in China to the retrieval of past global changes—some problems. *Physics of the Earth and Planetary Interiors* **70**, 154–168.

IUSS Working Group WRB, 2022. *World Reference Base for Soil Resources. International Soil Classification System for Naming Soils and Creating Legends for Soil Maps*. 4th ed. International Union of Soil Sciences (IUSS), Vienna.

Jary, Z., 2007. *Zapis Zmian Klimatu w Gornoplejstocenskich Sekwencjach Lessowo-Glebowych w Polsce i w Zahodniej Czesci Ukrainy*. Instytut Geografii i Rozwoju Regionalnego Uniwersytetu Wroclawskiego, Wroclaw.

Jary, Z., 2009. Periglacial markers within the Late Pleistocene loess–palaeosol sequences in Poland and Western Ukraine. *Quaternary International* **198**, 124–135.

Jary, Z., Ciszek, D., 2013. Late Pleistocene loess–palaeosol sequences in Poland and western Ukraine. *Quaternary International* **296**, 37–50.

Jordanova, D., Jordanova, N., 2021. Updating the significance and paleoclimate implications of magnetic susceptibility of Holocene loessic soils. *Geoderma* **391**, 114982. https://doi.org/10.1016/j.geoderma.2021.114982.

Jordanova, D., Laag, C., Jordanova, N., Lagroix, F., Georgieva, B., Ishlyamski, D., Guyodo, Y., 2022. A detailed magnetic record of Pleistocene climate and distal ash dispersal during the last 800 kyrs – the Suhia Kladenetz quarry loess-paleosol sequence near Pleven (Bulgaria). *Global and Planetary Change* **214**, 103840. https://doi.org/10.1016/j.gloplacha.2022.103840.

Jordanova, D., Petersen, N., 1999. Palaeoclimatic record from a loess–soil profile in northeastern Bulgaria—I. Rock magnetic properties. *Geophysical Journal International* **138**, 520–532.

Kachynskyi, N.A., 1958. *Grain-size and Microaggregate Composition of Soil, Methods for its Study*. [In Russian.] AS USSR, *Moscow*.

Kemp, R.A., 2001. Pedogenic modification of loess: significance for palaeoclimatic reconstructions. *Earth-Science Reviews* **54**, 145–156.

Költringer, C., Bradák, B., Stevens, T., Almqvist, B., Banak, A., Lindner, M., Kurbanov, R., Snowball, I., 2021a. Palaeoenvironmental implications from Lower Volga loess – joint magnetic fabric and multi-proxy analyses. *Quaternary Science Reviews* **267**, 107057. https://doi.org/10.1016/j.quascirev.2021.107057.

Költringer, C., Stevens, T., Bradák, B., Almqvist, B., Kurbanov, R., Snowball, I., Yarovaya, S., 2021b. Enviromagnetic study of Late Quaternary environmental evolution in Lower Volga loess sequences, Russia. *Quaternary Research* **103**, 49–73.

Komar, M., Łanczont, M., Fedorowicz, S., Gozhik, P., Mroczek, P., Bogucki, A., 2018. Stratigraphic interpretation of loess in the marginal zone of the Dnieper I ice sheet and the evolution of its landscape after deglaciation (Dnieper Upland, Ukraine). *Geological Quarterly* **62**, 536–552.

Komar, M., Łanczont, M., Madeyska, T., 2009. Spatial vegetation patterns based on palynological records in the loess area between the Dnieper and Odra Rivers during the last interglacial–glacial cycle. *Quaternary International* **198**, 152–172.

Komar, M., Łanczont, M., Madeyska, T., 2015. Vegetation of the Palaeolithic ecumene of the Peric and Metacarpathic zones. In: Łanczont, M., Madeyska, T. (Eds.), *Paleolityczna Ekumena Strefy Pery- i Metakarpackiej*. [In Polish.] Wydawnictwo Uniwersytetu Marii Curie-Sklodowskiej, Lublin, pp. 489–557.

Konishchev, V.N., Rogov, V.V., 1977. Micromorphology of cryogenic soils and subsoils. [In Russian.] *Pochvovedenie* **2**, 119–125.

https://doi.org/10.1017/qua.2024.51 Published online by Cambridge University Press

Kühn, P., Aguilar, J., Miedema, R., Bronnikova, M., 2018. Textural pedofeatures and related horizons. In: Stoops, G., Marcelino, V., Mees, F. (Eds.), *Interpretation of Micromorphological Features of Soils and Regoliths (Second Edition)*. Elsevier, Amsterdam, pp. 377–423.

Kukla, G.J., 1977. Pleistocene land–sea correlations I. Europe. *Earth-Science Reviews* **13**, 307–374.

Kukla, G., An, Z., 1989. Loess stratigraphy in Central China. *Palaeogeography, Palaeoclimatology, Palaeoecology* **72**, 203–225.

Kukla, G., Cílek, V., 1996. Plio-Pleistocene megacycles: record of climate and tectonics. *Palaeogeography, Palaeoclimatology, Palaeoecology* **120**, 171–194.

Kusiak, J., Łanczont, M., Bogucki, A.B., 2012. New exposure of loess deposits in Boyanychi (Ukraine) — results of thermoluminescence analyses. *Geochronometria* **39**, 84–100.

Laag, C., Hambach, U., Zeeden, C., Lagroix, F., Guyodo, Y., Veres, D., Jovanović, M., Marković, S.B., 2021. A detailed paleoclimate proxy record for the Middle Danube Basin over the last 430 kyr: a rock magnetic and colorimetric study of the Zemun loess-paleosol sequence. *Frontiers in Earth Science* **9**, 600086. https://doi.org/10.3389/feart.2021.600086.

Łącka, B., Łanczont, M., Madeyska, T., Bogutsky, A., 2007. Geochemical composition of Vistulian loess and micromorphology of interstadial palaeosols at the Kolodiiv site (East Carpathian Foreland, Ukraine). *Geological Quarterly* **51**, 127–146.

Łanczont, M., Bogutsky, A., 2007. High-resolution terrestrial archive of climatic oscillations during Oxygen Isotope Stages 5-2 in the loess-palaeosol sequence at Kolodiiv (East Carpathian Foreland, Ukraine). *Geological Quarterly* **51**, 105–126.

Łanczont, M., Fedorowicz, S., Kusiak, J., Boguckij, A., Sytnyk, O., 2009. TL age of loess deposits in the Yezupil I Palaeolithic site on the upper Dniester River (Ukraine). *Geologija* **51**, 86–96.

Łanczont, M., Komar, M., Madeyska, T., Mroczek, P., Standzikowski, K., Hołub, B., Fedorowicz, S., *et al.*, 2022. Spatio-temporal variability of topoclimates and local palaeoenvironments in the Upper Dniester River Valley: insights from the Middle and Upper Palaeolithic key-sites of the Halych region (western Ukraine). *Quaternary International* **632**, 112–131.

Łanczont, M., Madeyska, T., 2015. *Paleolityczna Ekumena Strefy Pery- i Metakarpackiej*. Wydawnictwo Uniwersytetu Marii Curie-Sklodowskiej, Lublin.

Łanczont, M., Madeyska, T., Mroczek, P., Komar, M., Hołub, B., Standzikowski, K., Fedorowicz, S., 2023. Reconstruction of the environmental conditions during the earliest Palaeolithic occupations in the Podillia Upland (W Ukraine) and the formation of archaeological layers. *Catena* **221**, 106753. https://doi.org/10.1016/j.catena.2022.106753.

Łanczont, M., Madeyska, T., Sytnyk, O., Bogucki, A., Komar, M., Nawrocki, J., Hołub, B., Mroczek, P., 2015. Natural environment of MIS 5 and soil catena sequence along a loess slope in the Seret River valley: evidence from the Pronyatyn Palaeolithic site (Ukraine). *Quaternary International* **365**, 74–97.

Łanczont, M., Sytnyk, O., Bogucki, A., Madeyska, T., Krajcarz, M., Krajcarz, M.T., Koropeckyj, R., Żogała, B., Tomek, T., Kusiak, J., 2014. Character and chronology of natural events modifying the Palaeolithic settlement records in the Ihrovytsia site (Podolia, the Ukraine). *Quaternary International* **326–327**, 213–234.

Lehmkuhl, F., Nett, J.J., Pötter, S., Schulte, P., Sprafke, T., Jary, Z., Antoine, P., *et al.*, 2021. Loess landscapes of Europe – mapping, geomorphology, and zonal differentiation. *Earth-Science Reviews* **215**, 103496. https://doi.org/10.1016/j.earscirev.2020.103496.

Li, Y., Shi, W., Aydin, A., Beroya-Eitner, M.A., Gao, G., 2020. Loess genesis and worldwide distribution. *Earth-Science Reviews* **201**, 102947. https://doi.org/10.1016/j.earscirev.2019.102947.

Lindner, L., Bogutsky, A., Gozhik, P., Marks, L., Łanczont, M., Wojtanowicz, J., 2006. Correlation of Pleistocene deposits in the area between the Baltic and Black Sea, Central Europe. *Geological Quarterly* **50**, 195–210.

Lisiecki, L.E., Raymo, M.E., 2005. A Pliocene-Pleistocene stack of 57 globally distributed benthic $\delta^{18}O$ records. *Paleoceanography* **20**, PA1003. https://doi.org/10.1029/2004PA001071.

Liu, Q., Roberts, A.P., Larrasoaña, J.C., Banerjee, S.K., Guyodo, Y., Tauxe, L., Oldfield, F., 2012. Environmental magnetism: principles and applications. *Reviews of Geophysics* **50**. https://doi.org/10.1029/2012RG000393

Liu, T.S., 1985. *Loess and the Environment*. Science Press, Beijing.

Liu, X.M., Hesse, P., Rolph, T., Begét, J.E., 1999. Properties of magnetic mineralogy of Alaskan loess: evidence for pedogenesis. *Quaternary International* **62**, 93–102.

Liu, X.M., Mao, X.G., 2021. Loess-palaeosol sequences in diverse environments: aeolian accumulation identification and magnetic susceptibility models. *Palaeogeography, Palaeoclimatology, Palaeoecology* **584**, 110683. https://doi.org/10.1016/j.palaeo.2021.110683.

Lowe, J.J., Walker, M., 2014. *Reconstructing Quaternary Environments*. 3rd ed. Routledge, London.

Ma, M., Liu, X., Hesse, P.P., Lü, B., Guo, X., Chen, J., 2013. Magnetic properties of loess deposits in Australia and their environmental significance. *Quaternary International* **296**, 198–205.

Maher, B.A., 1998. Magnetic properties of modern soils and Quaternary loessic paleosols: paleoclimatic implications. *Palaeogeography, Palaeoclimatology, Palaeoecology* **137**, 25–54.

Maher, B.A., 2016. Palaeoclimatic records of the loess/palaeosol sequences of the Chinese Loess Plateau. *Quaternary Science Reviews* **154**, 23–84.

Maher, B.A., Alekseev, A., Alekseeva, T., 2003. Magnetic mineralogy of soils across the Russian Steppe: climatic dependence of pedogenic magnetite formation. *Palaeogeography, Palaeoclimatology, Palaeoecology* **201**, 321–341.

Maher, B.A., Thompson, R., 1992. Paleoclimatic significance of the mineral magnetic record of the Chinese loess and paleosols. *Quaternary Research* **37**, 155–170.

Makeev, A., Rusakov, A., Kust, P., Lebedeva, M., Khokhlova, O., 2024. Loess-paleosol sequence and environmental trends during the MIS5 at the southern margin of the Middle Russian Upland. *Quaternary Science Reviews* **328**, 108372. https://doi.org/10.1016/j.quascirev.2023.108372.

Mamakowa, K., 1989. Late Middle Polish Glaciation, Eemian and Early Vistulian vegetation at Imbramowice near Wrocław and the pollen stratigraphy of this part of the Pleistocene in Poland. *Acta Palaeobotanica* **29**, 11–176.

Marković, S.B., Bokhorst, M.P., Vandenberghe, J., McCoy, W.D., Oches, E.A., Hambach, U., Gaudenyi, T., *et al.*, 2008. Late Pleistocene loess-palaeosol sequences in the Vojvodina region, north Serbia. *Journal of Quaternary Science* **23**, 73–84.

Marković, S.B., Hambach, U., Stevens, T., Kukla, G.J., Heller, F., McCoy, W.D., Oches, E.A., Buggle, B., Zöller, L., 2011. The last million years recorded at the Stari Slankamen (Northern Serbia) loess-palaeosol sequence: revised chronostratigraphy and long-term environmental trends. *Quaternary Science Reviews* **30**, 1142–1154.

Marković, S.B., Hughes, P.D., Schaetzl, R., Gibbard, P.L., Hao, Q., Radaković, M.G., Vandenberghe, J., *et al.*, 2024. The relationship between the loess stratigraphy in the Vojvodina region of northern Serbia and the Saalian and Rissian Stage glaciations – a review. *Boreas* **53**, 577–592.

Marković, S.B., Stevens, T., Kukla, G.J., Hambach, U., Fitzsimmons, K.E., Gibbard, P., Buggle, B., *et al.*, 2015. Danube loess stratigraphy—towards a pan-European loess stratigraphic model. *Earth-Science Reviews* **148**, 228–258.

Marković, S.B., Sümegi, P., Stevens, T., Schaetzl, R.J., Obreht, I., Chu, W., Buggle, B., *et al.*, 2018. The Crvenka loess-paleosol sequence: a record of continuous grassland domination in the southern Carpathian Basin during the Late Pleistocene. *Palaeogeography, Palaeoclimatology, Palaeoecology* **509**, 33–46.

Marks, L., 2023. Pleistocene glaciations in southern Poland – a revision. *Geological Quarterly* **67**, 67–25.

Matoshko, A.V., 2011. Limits of the Pleistocene glaciations in the Ukraine: a closer look. In: Ehlers, J., Gibbard, P.L., Hughes, P.D. (Eds.), *Developments in Quaternary Sciences Vol. 15, Quaternary Glaciations – Extent and Chronology*. Elsevier, Amsterdam, pp. 405–418.

Matoshko, A., 2021. Loess and its derivatives in a common sedimentary and geomorphic evolution of the East European Plain. *Aeolian Research* **53**, 100750. https://doi.org/10.1016/j.aeolia.2021.100750.

Matsuoka, N., 2001. Solifluction rates, processes and landforms: a global review. *Earth-Science Reviews* **55**, 107–134.

Matviishyna, Z., Kushnir, A., 2021. Climatic and landscape influences on the distribution and abundance of the Pleistocene small-mammal burrows of Ukraine. *Historical Biology* **33**, 97–108.

https://doi.org/10.1017/qua.2024.51 Published online by Cambridge University Press

Matviishyna, Z.M., Gerasimenko, N.P., Perederyi, V.I., Bragin, A.M., Ivchenko, A.S., Karmazinenko, S.P., Nagirnyi, V.M., Parkhomenko, O.G., 2010. *Spatio-Temporal Correlation of Quaternary Palaeogeographic Conditions on the Territory of Ukraine*. [In Ukrainian.] Naukova Dumka, Kyiv.

Matviishyna, Zh.N., 1982. *Micromorphology of the Pleistocene Soils of Ukraine*. [In Russian.] Naukova Dumka, *Kyiv*.

Maxbauer, D.P., Feinberg, J.M., Fox, D.L., 2016. Magnetic mineral assemblages in soils and paleosols as the basis for paleoprecipitation proxies: a review of magnetic methods and challenges. *Earth-Science Reviews* **155**, 28–48.

Morozova, T.D., 1981. *Soil Cover Development in Europe in the Late Pleistocene*. [In Russian.] Nauka, Moscow.

Moska, P., Adamiec, G., Jary, Z., Bluszcz, A., 2017. OSL chronostratigraphy for loess deposits from Tyszowce – Poland. *Geochronometria* **44**, 307–318.

Moska, P., Jary, Z., Adamiec, G., Bluszcz, A., 2019. Chronostratigraphy of a loess-palaeosol sequence in Biały Kościół, Poland using OSL and radiocarbon dating. *Quaternary International* **502**, 4–17.

Mroczek, P., 2013. Recycled loesses – a micromorphological approach to the determination of local source areas of Weichselian loess. *Quaternary International* **296**, 241–250.

Muhs, D.R., Ager, T.A., Bettis, E.A., McGeehin, J., Been, J.M., Begét, J.E., Pavich, M.J., Stafford, T.W., Stevens, D.A.S.P., 2003. Stratigraphy and palaeoclimatic significance of Late Quaternary loess–palaeosol sequences of the Last Interglacial–Glacial cycle in central Alaska. *Quaternary Science Reviews* **22**, 1947–1986.

Munsell Color, 2009. *Munsell Soil-Color Charts*. Munsell Color, Grand Rapids, MI, USA.

Namier, N., Gao, X., Hao, Q., Marković, S.B., Fu, Y., Song, Y., Zhang, H., *et al.*, 2021. Mineral magnetic properties of loess–paleosol couplets of northern Serbia over the last 1.0 Ma. *Quaternary Research* **103**, 35–48.

NASA Shuttle Radar Topography Mission (SRTM), 2013. Shuttle Radar Topography Mission (SRTM) Global. Distributed by Open Topography. https://doi.org/10.5069/G9445JDF.

Nawrocki, J., 1992. Magnetic susceptibility of Polish loesses and loess-like sediments. *Geologica Carpathica* **43**, 179–180.

Nawrocki, J., Bakhmutov, V., Bogucki, A., Dolecki, L., 1999. The paleo- and petromagnetic record in the Polish and Ukrainian loess-paleosol sequences. *Physics and Chemistry of the Earth, Part A: Solid Earth and Geodesy* **24**, 773–777.

Nawrocki, J., Bogucki, A., Łanczont, M., Nowaczyk, N.R., 2002. The Matuyama–Brunhes boundary and the nature of magnetic remanence acquisition in the loess–palaeosol sequence from the western part of the East European loess province. *Palaeogeography, Palaeoclimatology, Palaeoecology* **188**, 39–50.

Nawrocki, J., Bogucki, A., Łanczont, M., Werner, T., Standzikowski, K., Pańczyk, M., 2018. The Hilina Pali palaeomagnetic excursion and possible self-reversal in the loess from western Ukraine. *Boreas* **47**, 954–966.

Nawrocki, J., Bogutsky, A., Łanczont, M., 2007. Palaeomagnetic studies of the loess-palaeosol sequence from the Kolodiiv section (East Carpathian Foreland, Ukraine). *Geological Quarterly* **51**, 161–166.

Nawrocki, J., Polechońska, O., Boguckij, A., Łanczont, M., 2006. Palaeowind directions recorded in the youngest loess in Poland and western Ukraine as derived from anisotropy of magnetic susceptibility measurements. *Boreas* **35**, 266–271.

Nawrocki, J., Wøjcik, A., Bogucki, A., 1996. The magnetic susceptibility record in the Polish and western Ukrainian loess-palaeosol sequences conditioned by palaeoclimate. *Boreas* **25**, 161–169.

Nechaev, V.P., 1983. Paleocryogenic Processes in the Volyn-Podollia Upland in the Upper Pleistocene. [In Russian.] PhD thesis, Institute of Geography, Academy of Sciences USSR, Moscow.

Osadchyi, V., Skrynyk, O., Palamarchuk, L., Skrynyk, O., Osypov, V., Oshurok, D., Sidenko, V., 2022. Dataset of gridded time series of monthly air temperature (min, max, mean) and atmospheric precipitation for Ukraine covering the period of 1946–2020. *Data in Brief* **44**, 108553. https://doi.org/10.1016/j.dib.2022.108553.

Panaiotu, C.G., Panaiotu, E.C., Grama, A., Necula, C., 2001. Paleoclimatic record from a loess-paleosol profile in southeastern Romania. *Physics and Chemistry of the Earth, Part A: Solid Earth and Geodesy* **26**, 893–898.

Pécsi, M., 1990. Loess is not just the accumulation of dust. *Quaternary International* **7–8**, 1–21.

Pye, K., 1995. The nature, origin and accumulation of loess. *Quaternary Science Reviews* **14**, 653–667.

Rasmussen, S.O., Bigler, M., Blockley, S.P., Blunier, T., Buchardt, S.L., Clausen, H.B., Cvijanovic, I., *et al.*, 2014. A stratigraphic framework for abrupt climatic changes during the Last Glacial period based on three synchronized Greenland ice-core records: refining and extending the INTIMATE event stratigraphy. *Quaternary Science Reviews* **106**, 14–28.

Romanovskiy, N.N., 1993. *Basics of Lithosphere Cryogenesis*. [In Russian.] Moscow University, Moscow.

Rose, J., Lee, J.A., Kemp, R.A., Harding, P.A., 2000. Palaeoclimate, sedimentation and soil development during the Last Glacial Stage (Devensian), Heathrow Airport, London, UK. *Quaternary Science Reviews* **19**, 827–847.

Rousseau, D.-D., Antoine, P., Boers, N., Lagroix, F., Ghil, M., Lomax, J., Fuchs, M., *et al.*, 2020. Dansgaard–Oeschger-like events of the penultimate climate cycle: the loess point of view. *Climate of the Past* **16**, 713–727.

Rousseau, D.-D., Antoine, P., Gerasimenko, N., Sima, A., Fuchs, M., Hatté, C., Moine, O., Zoeller, L., 2011. North Atlantic abrupt climatic events of the last glacial period recorded in Ukrainian loess deposits. *Climate of the Past* **7**, 221–234.

Rousseau, D.-D., Gerasimenko, N., Matviischina, Z., Kukla, G., 2001. Late Pleistocene environments of the Central Ukraine. *Quaternary Research* **56**, 349–356.

Rousseau, D.-D., Ghil, M., Kukla, G., Sima, A., Antoine, P., Fuchs, M., Hatté, C., Lagroix, F., Debret, M., Moine, O., 2013. Major dust events in Europe during marine isotope stage 5 (130-74 ka): a climatic interpretation of the "markers." *Climate of the Past* **9**, 2213–2230.

Sartori, M., Heller, F., Forster, T., Borkovec, M., Hammann, J., Vincent, E., 1999. Magnetic properties of loess grain size fractions from the section at Paks (Hungary). *Physics of the Earth and Planetary Interiors* **116**, 53–64.

Sharyfulina, R.A., Behal, O.S., Olenchuk, Ya.S., Vysotska, T.A., Metel, K.Ye., Kaplan, G.N., Yeremeeva, M.Ya., Nahorna, V.N., 1967. Soil map of the Ukrainian SSR. Sheet 33, scale: 1:200 000. In: Krupskyi, M.K. (Ed.), *Soil Map of the Ukrainian SSR*. [In Ukrainian.] Ukrainian Research Institute of Soil Science named after A.N. Sokolovsky, Republican Design Institute for Land Management "UKRZEMPROEKT".

Solleiro-Rebolledo, E., Cabadas, H., Terhorst, B., 2013. Paleopedological record along the loess-paleosol sequence in Oberlaab, Austria. *E&G Quaternary Science Journal* **62**, 22–33.

Sprafke, T., Terhorst, B., Peticzka, R., Thiel, C., 2013. Paudorf locus typicus (Lower Austria) revisited: the potential of the classic loess outcrop for Middle to Late Pleistocene landscape reconstructions. *E&G Quaternary Science Journal* **62**, 59–72.

Sprafke, T., Thiel, C., Terhorst, B., 2014. From micromorphology to palaeoenvironment: the MIS 10 to MIS 5 record in Paudorf (Lower Austria). *Catena* **117**, 60–72.

Stoops, G., 2003. *Guidelines for Analysis and Description of Soil and Regolith Thin Sections*. Soil Science Society of America, Madison, WI, USA.

Stoops, G., Marcelino, V., Mees, F., 2018. *Interpretation of Micromorphological Features of Soils and Regoliths (Second Edition)*. Elsevier, Amsterdam.

Sümegi, P., Gulyás, S., Molnár, D., Sümegi, B.P., Almond, P.C., Vandenberghe, J., Zhou, L., *et al.*, 2018. New chronology of the best developed loess/paleosol sequence of Hungary capturing the past 1.1 ma: implications for correlation and proposed pan-Eurasian stratigraphic schemes. *Quaternary Science Reviews* **191**, 144–166.

Sycheva, S., Frechen, M., Terhorst, B., Sedov, S., Khokhlova, O., 2020. Pedostratigraphy and chronology of the Late Pleistocene for the extra glacial area in the Central Russian Upland (reference section Aleksandrov quarry). *Catena* **194**, 104689. https://doi.org/10.1016/j.catena.2020.104689.

Tecsa, V., Gerasimenko, N., Veres, D., Hambach, U., Lehmkuhl, F., Schulte, P., Timar-Gabor, A., 2020. Revisiting the chronostratigraphy of Late Pleistocene loess-paleosol sequences in southwestern Ukraine: OSL dating of Kurortne section. *Quaternary International* **542**, 65–79.

Terhorst, B., Appel, E., Werner, A., 2001. Palaeopedology and magnetic susceptibility of a loess–palaeosol sequence in southwest Germany. *Quaternary International* **76–77**, 231–240.

Trask, P.D., 1932. *Origin and Environment of Source Sediments of Petroleum*. Gulf Publishing Co, Houston.

https://doi.org/10.1017/qua.2024.51 Published online by Cambridge University Press

Tsatskin, A., Gendler, T.S., Heller, F., 2008. Improved paleopedological reconstruction of Vertic paleosols at Novaya Etuliya, Moldova via integration of soil micromorphology and environmental magnetism. In: Kapur, S., Mermut, A., Stoops, G. (Eds.), *New Trends in Soil Micromorphology*. Springer, Berlin, Heidelberg, pp. 91–110.

Tsatskin, A., Heller, F., Hailwood, E.A., Gendler, T.S., Hus, J., Montgomery, P., Sartori, M., Virina, E.I., 1998. Pedosedimentary division, rock magnetism and chronology of the loess/palaeosol sequence at Roxolany (Ukraine). *Palaeogeography, Palaeoclimatology, Palaeoecology* **143**, 111–133.

Van Loon, A.J., 2006. Lost loesses. *Earth-Science Reviews* **74**, 309–316.

Van Vliet-Lanoë, B., Fox, C.A., 2018. Frost action. In: Stoops, G., Marcelino, V., Mees, F. (Eds.), *Interpretation of Micromorphological Features of Soils and Regoliths (Second Edition)*. Elsevier, Amsterdam, pp. 575–603.

Van Vliet-Lanoë, B., Van Brulhet, J., Combes, P., Duvail, C., Ego, F., Baize, S., Cojan, I., 2017. Quaternary thermokarst and thermal erosion features in northern France: origin and palaeoenvironments. *Boreas* **46**, 442. https://doi.org/10.1111/bor.12221.

Veklych, M.F., 1968. *Stratigraphy of the Loess of Ukraine and Adjacent Countries*. [In Russian.] Naukova Dumka, Kyiv.

Veklych, M.F., 1982. *Stages and Stratotypes of the Soil Formations of Ukraine in the Upper Cenozoic*. [In Russian.] Naukova Dumka, Kyiv.

Veklych, M.F., Sirenko, N.A., Matviishyna, Z.N., Gerasimenko, N.P., Perederiy, V.I., Turlo, S.I., 1993. *The Pleistocene Stratigraphical Framework of the Ukraine*. [In Russian.] State Committee of Geology of Ukraine, Kyiv.

Veklych, M.F., Sirenko, N.A., Matviishyna, Z.N., Melnychuk, I.V., Perederyi, V.I., Turlo, S.I., Vozgrin, B.D., 1984. *Palaeogeographical Succession and Detailed Stratigraphic Division of the Pleistocene of Ukraine (Methodological Developments)*. [In Russian.] Naukova Dumka, Kyiv.

Verrecchia, E.P., Verrecchia, K.E., 1994. Needle-fiber calcite; a critical review and a proposed classification. *Journal of Sedimentary Research* **64**, 650–664.

Vigilyanskaya, L.I., 2002. Palaeomagnetic studies of Pliocene-Pleistocene deposits of loess-palaeosol stratum in Middle Dnieper region. [In Russian.] *Geofizicheskiy Zhurnal* **24**, 36–42.

Vozgrin, B.D., 2001. Problems of stratigraphic subdivision and correlation of terrestrial deposits of the Antropogene of Ukraine. In: *Regional Geological Studies in Ukraine and the Question of Creating a State Geologic Map*. [In Ukrainian.] The State Geological Survey, Ukrainian State Research Institute for Geological Survey, Kyiv, pp. 30–32.

Wacha, L., Laag, C., Grizelj, A., Tsukamoto, S., Zeeden, C., Ivanišević, D., Rolf, C., Banak, A., Frechen, M., 2021. High-resolution palaeoenvironmental reconstruction at Zmajevac (Croatia) over the last three glacial/interglacial cycles. *Palaeogeography, Palaeoclimatology, Palaeoecology* **576**, 110504. https://doi.org/10.1016/j.palaeo.2021.110504.

Wacha, L., Rolf, C., Hambach, U., Frechen, M., Galović, L., Duchoslav, M., 2018. The Last Glacial aeolian record of the Island of Susak (Croatia) as seen from a high-resolution grain-size and rock magnetic analysis. *Quaternary International* **494**, 211–224.

Wang, H., Lundstrom, C.C., Zhang, Z., Grimley, D.A., Balsam, W.L., 2009. A Mid–Late Quaternary loess–paleosol record in Simmons Farm in southern Illinois, USA. *Quaternary Science Reviews* **28**, 93–106.

Wolhfarth, B., 2013. A review of Early Weichselian climate (MIS 5d-a) in Europe. Technical Report TR-13-03. Stockholm University, Stockholm.

Zeeden, C., Hambach, U., 2021. Magnetic susceptibility properties of loess from the Willendorf Archaeological Site: implications for the syn/post-depositional interpretation of magnetic fabric. *Frontiers in Earth Science* **8**. https://doi.org/10.3389/feart.2020.599491.

Zhu, R.X., Matasova, G., Kazansky, A., Zykina, V., Sun, J.M., 2003. Rock magnetic record of the last glacial—interglacial cycle from the Kurtak loess section, southern Siberia. *Geophysical Journal International* **152**, 335–343.

Zöller, L., Fischer, M., Jary, Z., Antoine, P., Krawczyk, M., 2022. Chronostratigraphic and geomorphologic challenges of last glacial loess in Poland in the light of new luminescence ages. *E&G Quaternary Science Journal* **71**, 59–81.

https://doi.org/10.1017/qua.2024.51 Published online by Cambridge University Press